THESIS

LABORATORY EVALUATION OF A MICROFLUIDIC ELECTROCHEMICAL SENSOR FOR AEROSOL OXIDATIVE LOAD

Submitted by

Jeffrey Shapiro

Department of Environmental and Radiological Health Sciences

In partial fulfillment of the requirements

For the Degree of Master of Science

Colorado State University

Fort Collins, Colorado

Summer 2012

Master's Committee:

Advisor: John Volckens

Charles Henry
Jennifer Peel

ABSTRACT

LABORATORY EVALUATION OF A MICROFLUIDIC ELECTROCHEMICAL SENSOR FOR AEROSOL OXIDATIVE LOAD

Human exposure to particulate matter (PM) air pollution is associated with both human morbidity and mortality. The mechanisms by which PM impacts human health are yet unresolved, but evidence suggests that PM intake leads to cellular oxidative stress through the generation of reactive oxygen species (ROS). Therefore, reliable tools are needed for estimating the oxidant generating capacity, or oxidative load, of PM. The most widely reported method for assessing PM oxidative load is the dithiothreitol (DTT) assay. The traditional DTT assay utilizes filter-based PM collection in conjunction with laboratory analysis. However, the traditional DTT assay suffers from poor time resolution, loss of reactive species during sampling, and high limit of detection. Recently, a new DTT assay was developed by coupling a Particle Into Liquid Sampler with microfluidic-electrochemical detection. This 'on-line' system allows continuous monitoring of PM reactivity (~three minute measurement resolution) from substantially reduced sample masses (nanograms). This study reports on a laboratory evaluation of the on-line DTT approach. A standard urban dust sample was aerosolized in a laboratory test chamber at three atmospherically-relevant concentrations allowing comparison of the on-line and traditional DTT methods. The on-line system gave a stronger correlation between DTT consumption rate and PM mass (R^2 = 0.93) than the traditional method (R^2 = 0.29). The on-line system also reported ~1.4 times greater relative reactivity for a given PM sample compared to the traditional method (p = 0.022) indicating improved efficiency for the capture and detection of redox-active species. These results suggest that on-line methods for PM sampling and reactivity analysis may improve our ability to study impacts of PM exposure on human health.

TABLE OF CONTENTS

DEFINITIONS

ANS – Autonomic Nervous System

CMD – Count Median Diameter

CoPC – Cobalt(II) phthalocyanine

d_{ae} – Aerodynamic diameter; the geometric diameter of a sphere with the same settling velocity as the particle of interest

d_m – Mobility diameter; the geometric diameter of a sphere with the same mobility in a constant electric field as the particle of interest

DCFH – Dichlorofluorescein

DI – De-ionized

DTNB – 5,5'-dithibis-2-nitrobenzoic, otherwise known as Ellman's reagent

DTT – Dithiothreitol

EDTA – Ethylenediaminetetraacetic acid

Electrochemistry – Branch of chemistry that analyzes oxidation/reduction reactions using electrodes to monitor electron transfer between reagents.

F^- – Fluoride ion

Fenton Chemistry – Electron transfer reactions in which catalytically reactive metals decompose hydrogen peroxide generating hydroxyl radicals in solution

GSD – Geometric Standard Deviation

HEPA – High Efficiency Particulate Air

IC – Ion Chromatography

LOD – Limit of Detection

Microfluidics – Branch of chemistry that performs reactions in micro-volumes

NaF – Sodium Fluoride

NIST SRM – National Institute of Standards and Technology Standard Reference Material

Cellular Oxidative Stress – Overwhelming of cellular defense mechanisms against reactive species, an altered redox-status

PAH – Polycyclic Aromatic Hydrocarbon

PVC – Polyvinyl Chloride

PDMS – Poly(Dimethylsiloxane)

PM – Particulate Matter

PILS – Particle Into Liquid Sampler

ROS – Reactive Oxygen Species

SE – Standard Error

SMPS – Sequential Mobility Particle Sizer

TNB – 5-mercapto-2-nitrobenzoic acid

UV/VIS – Ultraviolet/Visible light

Introduction

Extensive research has established a link between airborne particulate matter (PM) exposure and increased morbidity and mortality in humans (Mauderly and Chow 2008; Schlesinger 2007). Epidemiologic evidence has associated PM exposure with health outcomes including myocardial infarction (Brook et al. 2010; Peters et al. 2001), asthma (Li et al. 2003a), birth defects (Ritz et al. 2002), and lung cancer death (Dockery et al. 1993). Toxicological studies in animals and humans have observed elevations in cardiorespiratory inflammation (Becher et al. 2007; Fujii et al. 2002; Nurkiewicz et al. 2006), immune response (Becher et al. 2007; van Eeden et al. 2001; Mutlu et al. 2007; Tamagawa et al. 2008), and autonomic nervous system (ANS) imbalance (Ghelfi et al. 2008; Rhoden et al. 2005) resulting from both short and long-term PM exposure. Mechanisms by which PM induces ill-effects are unclear, yet evidence suggests multiple pathways. Proposed mechanisms include PM interference with lung receptors and nerves leading to ANS dysfunction (Stone and Godleski 1999; Timonen et al. 2006; Watkinson et al. 1998), ultrafine particle diffusion across alveolar membranes into bloodstream circulation (Nemmar et al. 2002), and excess generation of reactive oxygen species (ROS) by redox-active PM components (Sioutas et al. 2005; Squadrito et al. 2001) triggering a state of cellular oxidative stress (Schafer and Buettner 2001). All proposed mechanisms lead to excess ROS generation preceding oxidative stress in cells (Brook et al. 2010). Prolonged oxidative stress conditions can ultimately result in a cascade of inflammatory events leading to cellular damage, cell death, and subsequent disease (Brook et al. 2010; Li et al. 2002).

The oxidative stress mechanism is of particular interest for environmental health due to the physiochemical nature of typical atmospheric PM. On a particle number basis, PM exposures

in populated areas are generally dominated by ultrafine particles (aerodynamic diameter, d_{ae}<100μm) (Fine et al. 2004; Kim et al. 2002). Ultrafine particles likely introduce more cellular ROS per unit than larger PM sizes due to high efficiency deposition in the deep lungs, high particle numbers, and subsequently large total surface area (Sioutas et al. 2005). Particle surface chemistry further suggests PM triggers cellular oxidative stress via excess ROS generation. Typical environmental PM is a complex mixture of redox-active chemicals known to participate in various electron-transfer reactions (Kumagai et al. 1997; Veronesi et al. 1999; Wu et al. 1999). Many of these chemical species have been shown to produce ROS both in vitro and in vivo (Alessandrini et al. 2009; Vidrio et al. 2009). Transition metals like Fe, V, Cu, Zn, and Cr, are present in aerosols and generate cellular ROS via Fenton chemistry (Aust et al. 2002; Prousek 2007). Atmospheric PM also contains organic compounds known to induce cellular oxidative stress through ROS generation such as polycyclic aromatic hydrocarbons (PAH's) and quinones (Cho et al. 2005; Chung et al. 2006; Kumagai et al. 1997, 2002).

Therefore, a need exists for reliable measurement of PM redox activity (or oxidative load) to advance our understanding of the role PM plays in human disease (Chahine et al. 2007; Li et al. 2009a; Ntziachristos et al. 2007; De Vizcaya-Ruiz et al. 2006). Chemical assays offer potential for describing the oxidative load of PM (Bernardoni et al. 2011; Ichoku et al. 1999). The oldest chemical approaches analyzed chemical composition of PM to quantify species possessing redox-active moieties (Pöschl 2005). However, characterization of PM composition is costly, time consuming, and prone to measurement error, as not all redox-active species in PM are known. An alternative approach is to measure the redox activity of PM directly using solution-based methods. The most widely reported technique for measuring PM reactivity is the dithiothreitol (DTT) assay (Charrier and Anastasio 2012; Cho et al. 2005; Li et al. 2003b, 2009b;

De Vizcaya-Ruiz et al. 2006), in which the reduced form of DTT acts as a sentinel for ROS in solution. When PM is placed in solution, ROS released from or generated by the PM reacts with reduced DTT to form oxidized DTT (Figure 4). After a pre-determined time, the reaction is quenched and the remaining reduced DTT is developed with Ellman's reagent (5,5'-dithibis-2-nitrobenzoic or DTNB) to produce a yellow chromophore (5-mercapto-2-nitrobenzoic acid or TNB). This chromophore is then quantified with UV/VIS-spectroscopy at 412 nm. Change in absorbance over time is calculated and the oxidative load of the PM extract is reported in terms of DTT consumption rate (Cho et al. 2005). The DTT assay is considered biologically relevant because the rate of DTT consumption has been correlated with cellular oxidative stress *in vitro* (Li et al. 2003b) and because several components of ambient PM (e.g., redox-active quinones) have been shown to catalyze the generation of superoxide radicals from DTT in solution (Kumagai et al. 2002).

However, the traditional DTT method has significant limitations. The method requires expensive laboratory equipment that makes in-field analyses impractical. Spectrophotometric quantification of DTT requires the addition of quenching and developing reagents, which result in sample dilution and lowered detection limit. The traditional DTT approach, which relies on filter-based collection of PM, also requires relatively large sample masses (~100 µg per filter) and, thus, long sampling times (>24 hours) for typical atmospheres in the United States. This loss of temporal resolution hinders our ability to identify sources and events that are responsible for redox-active PM emissions. The time lag between sample collection and analysis also poses a problem as some redox-active PM components are highly volatile (half-lives ranging from seconds to minutes) and are likely lost during sample collection, transport, storage, and extraction (Foucaud et al. 2007; Hu et al. 2008). Extraction techniques used to separate particles

from filters can also alter PM composition and reactivity estimates. Solvent selection is problematic because the complex chemical constituents of atmospheric PM cover a wide range of solubilities and polarities. Different solvents are known to extract reactive compounds with varied efficiency, leading to inconsistent measures of DTT reactivity (Rattanavaraha et al. 2011; Truong et al. 2010). Moreover, many common solvents (i.e. dichloromethane, methanol, and dimethyl sulfoxide) pose significant health and safety risks for researchers.

Direct sampling and collection of PM into solution eliminates the need for filter collection, storage, and extraction. The Particle Into Liquid Sampler (PILS) (Orsini et al. 2003) performs efficient and rapid PM deposition into solution via steam condensation and impaction (Figure 6). The PILS is easily coupled with downstream instrumentation permitting on-line and on-site chemical analysis of ambient PM. The PILS has been successfully coupled with other PM characterization methods (Bateman et al. 2010; Sullivan et al. 2004) and produced results comparable to filter-based approaches. The Hopke group coupled a PILS with a dichlorofluorescein (DCFH) based assay for on-line characterization of particle-bound ROS (Venkatachari and Hopke 2008; Wang et al. 2011) pioneering an approach for on-line monitoring of PM redox activity. However, instability of the DCFH reagent due to photobleaching and photo-oxidation hindered the system's repeatability (Beer and Weber 1972; Wang et al. 2011) and poor temporal resolution (>20 minutes between samples) due to sample mass requirements prevented continuous observation of PM reactivity (Wang et al. 2011). Also, the system did not utilize an internal standard to account for sample dilution by the PILS (Venkatachari and Hopke 2008; Wang et al. 2011).

Recently, a novel electrochemical sensor for reduced DTT quantification was coupled to a PILS for on-line reactivity analysis (Sameenoi et al.). This technique employed cobalt(II)

phthalocyanine (CoPC) electrodes integrated within a microfluidic device for highly sensitive and selective quantification of reduced DTT in micro-volumes of solution (Figure 1). Compared with UV/VIS spectroscopy, CoPC electrodes improve detection of DTT by reducing the required sample masses (nanograms vs. micrograms) and reaction volumes (10 microliters vs. ~1 mL). CoPC electrodes are easily integrated within poly(dimethylsiloxane) (PDMS)–based microfluidic chips allowing for portable, inexpensive, and rapid monitoring of DTT consumption by PM (Garcia and Henry 2004; Jokerst et al.; Noblitt et al. 2009; Sameenoi et al.). Decreased sample mass and volume requirements permit improved temporal resolution (~three minutes between measurements) (Sameenoi et al., in press).

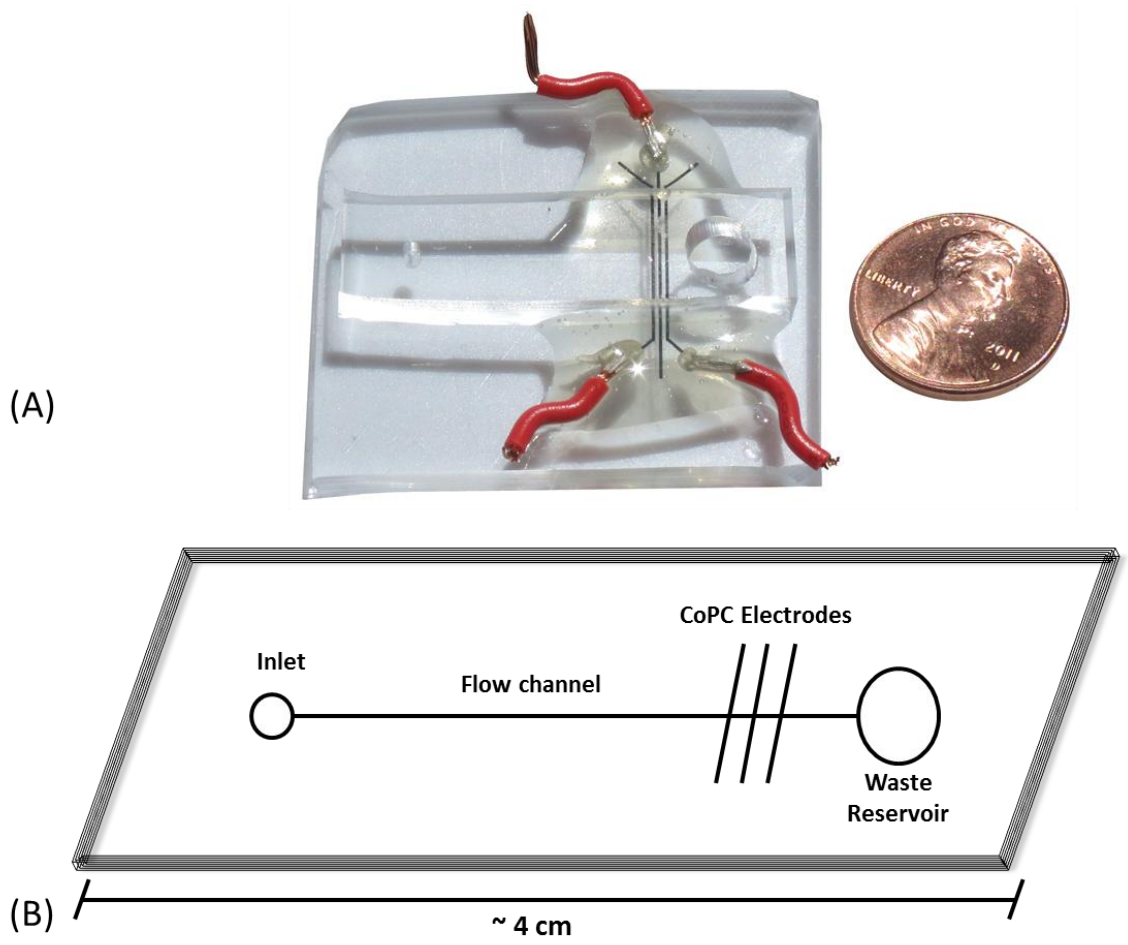

Figure 1: (A) Picture of a PDMS microfluidic chip infused with CoPC electrodes for sensing reduced DTT quantity in solution. (B) Chip schematic, 10 µL injections of the DTT+PM solution enters the inlet and is pushed through the flow channel by a syringe pump. CoPC electrodes measure electrical conductivity of the solution at a potential of +200 mV. Conductivity of the solution is directly proportional to DTT concentration.

This work represents a formal laboratory evaluation of the PILS-CoPC microfluidic chip system for monitoring oxidative load of PM (Sameenoi et al., accepted). A standard reference aerosol (NIST SRM 1649b, Washington D.C. Urban Dust) was generated at three atmospherically relevant concentrations (70, 30, 10 µg/m^3) within a ~1 m^3 test chamber to simulate typical PM exposures. Aerosol sampling and DTT reactivity analyses were performed in parallel to compare the traditional DTT method with the PILS-microfluidic approach. Oxidation of DTT is typically reported either as a raw rate (pmol DTT/minute) or a mass-

normalized rate (pmol DTT/minute/mass PM). Raw DTT consumption rate is linearly correlated with PM mass in the sample extract (Cho et al. 2005; Hu et al. 2008; Li et al. 2009a). Normalizing raw DTT consumption rate by PM mass produces a characteristic PM reactivity value across all masses. In this study, urban dust's DTT reactivity was reported both as a raw and mass-normalized consumption rate for each analysis technique. Based on previous work performed by Sameenoi *et al.*, we hypothesized that the on-line DTT system would *1) measure raw DTT consumption rate with a stronger linear correlation to PM mass than the traditional technique* and *2) detect a higher characteristic mass-normalized DTT consumption rate than the traditional technique*. The on-line system was expected to outperform the traditional approach by these metrics while also significantly reducing sample mass and improving temporal resolution.

Experimental Section

Chemicals and Materials

All reagents were obtained from Sigma-Aldrich (St. Louis, MO, USA). Electrochemical measurements were conducted using a commercially-available potentiostat (CHI812, CH Instruments, Austin, TX, USA) and UV/VIS absorbance measurements made with an absorbance spectrophotometer (MBA2000, Perkin Elmer Inc., Shelton, CT).

Experimental Setup

All PM sampling was performed within a ~1 m^3 acrylic test chamber at the Colorado State University Aerosol Technology Laboratory. The test chamber, a schematic is shown in Figure 2: was fitted with a desk fan, a dilution/exhaust manifold, and a timing switch to distribute PM evenly and to hold mass concentration steady during an experiment.

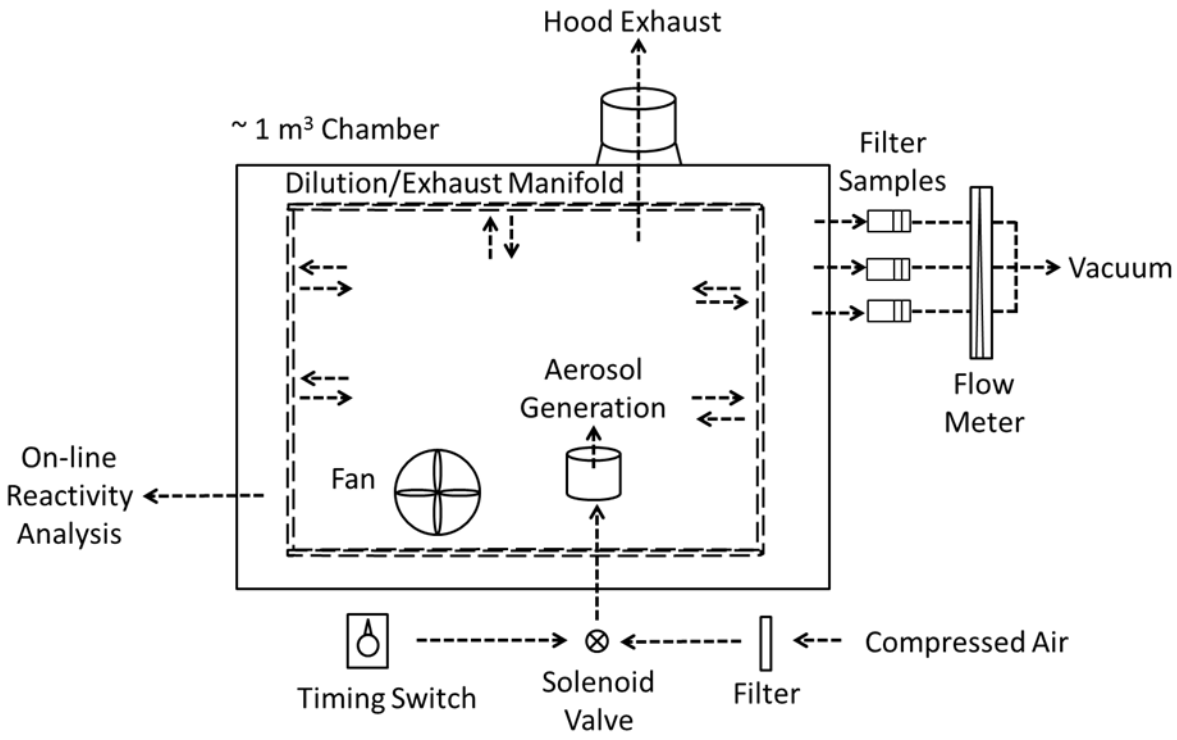

Figure 2: Schematic of experimental setup. Aerosolized urban dust was generated at high, middle, and low concentration levels within a controlled test chamber. A desk fan, dilution/exhaust manifold, and timing switch were installed to mix PM and hold mass concentration steady. Reactivity analysis was performed by both the traditional and on-line techniques in parallel for comparison.

The test aerosol, NIST SRM 1649b urban dust, is representative of PM typically found in urban air. This ultrafine PM sample is composed of chemical species correlated with DTT consumption including transition metals (Costa and Dreher 1997), PAH's, chlorinated pesticides, and polychlorinated biphenyl's (Wise and Watters 2009). Known masses of this dust sample were suspended in DI water (1% PM:H_20 by mass) and sonicated for 60 minutes to break apart agglomerates. The resultant suspension was aerosolized using a six-jet Collision Nebulizer (BGI, Waltham, MA). Aerosol was dispersed throughout the chamber by a small desk fan and diluted with filtered, compressed air supplied uniformly throughout the chamber.

Three PM concentration levels were investigated corresponding to high, middle, and low values (~70, 30, and 10 µg/m^3). Mass concentration within the chamber was monitored with a DustTrak (TSI, Shoreview, MN, USA) that was calibrated by a gravimetric reference sample. A dimensionless correction factor, K_g, was applied to calibrate DustTrak measurements to report actual (true) mass concentration using Eqn. (1):

$$K_G = \frac{\left[\frac{\sum_{i=1}^{n} D_i}{N}\right]}{F_G} \qquad \text{Eqn. (1)}$$

where D_i represents DustTrak mass concentration measurements (µg/m^3) taken at one minute intervals (i), N is the total number of DustTrak readings (180), and F_g is the mass concentration (µg/m^3) in the chamber determined by gravimetric analysis of a filter sample (as a time-weighted average). Time-resolved chamber mass concentration, C_i, was calculated by dividing the DustTrak signal by the correction factor using Eqn. (2):

$$C_i = \frac{D_i}{K_g} \qquad \text{Eqn. (2)}$$

Corrected concentrations values were used to calculate PM mass per injection for the PILS-Microfluidic system (see *On-line Reactivity Measurement*). Particle size distribution within the chamber was monitored using a Sequential Mobility Particle Sizer (SMPS) (Grimm Technologies, Douglasville, GA, USA) at regular intervals during each experiment.

Traditional DTT Method

PM Sampling and Handling

Urban dust was collected for 180 minutes onto 37 mm Teflon-coated glass fiber filters (Pall Corp., Port Washington, NY, USA). For high and middle concentration tests, filters were placed in closed-faced sampling cassettes and PM was sampled at 10 L/min. Low concentration tests required a higher sampling rate to collect sufficient sample mass. Therefore, sampling cassettes were used in an open-faced configuration and PM was collected at 20 L/min. Following gravimetric analysis, sample and blank filters were transferred into 15 mL centrifuge tubes and mixed with 3 mL methanol for extraction. Filter extracts were sonicated for 90 minutes and then cooled at room temperature for a minimum of 60 minutes. Extracts were then syringe filtered (Acrodisc Glass Fiber, 1 µm pore size, 25 mm diameter filter, Pall Corp., Port Washington, NY, USA) into a clean centrifuge tube and concentrated under nitrogen gas (N_2) to a final volume of ~2 mL. The N_2 concentration step increased sample mass per volume, which improved spectrophotometric detection of DTT under the traditional assay (Li et al. 2009b). Methanol was selected as the extraction solvent (vs. de-ionized water) for the following reasons: (1) methanol is reported to remove organic redox-active species more efficiently than de-ionized water for DTT analysis (Rattanavaraha et al. 2011) and most of the known reactive species in SRM 1649b are organic (Wise and Watters 2009); (2) we analyzed equal masses of urban dust extracted in separate methanol and DI water volumes and observed nearly double DTT consumption rate by methanol extract as shown in Figure 4; (3) methanol evaporates more quickly than water shortening handling time and minimizing volatile species losses.

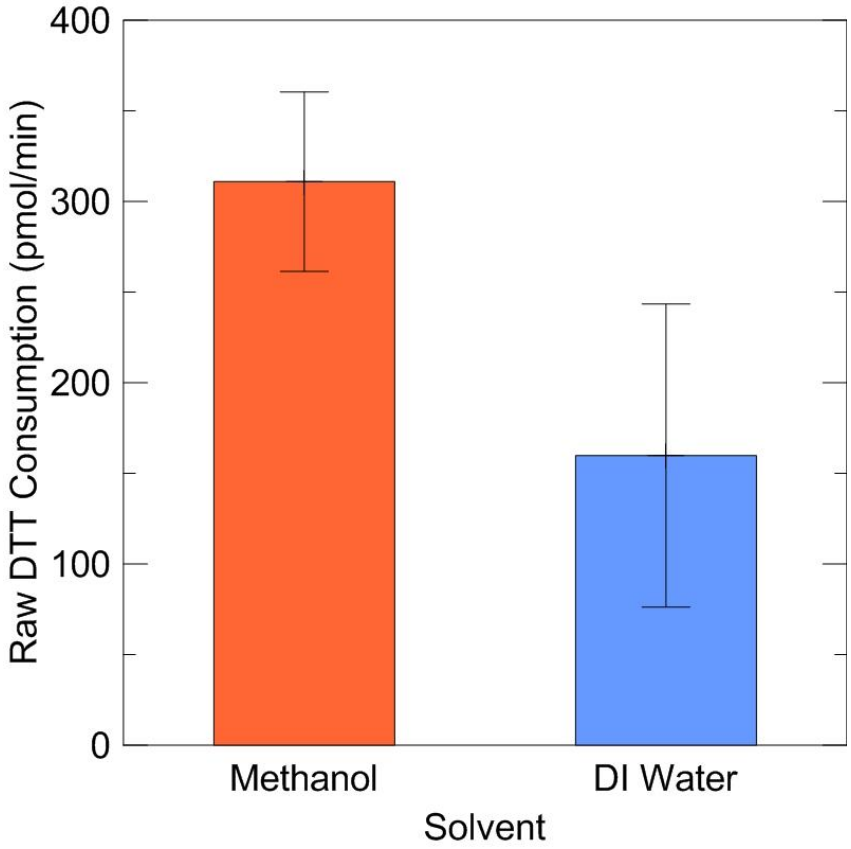

Figure 3: Bar chart comparing DTT reactivity of methanol and water-soluble fractions of SRM 1649b. Traditional DTT absorbance analysis was performed on methanol and water extracts containing 10 µg urban dust per assay. Extracts were assayed in triplicate and error bars indicate one standard deviation.

The mass of PM sample added to each assay, M_{assay}, was calculated from Eqn. (3):

$$M_{assay} = M_{total} \times (V_e - \frac{\Delta M_{extract}}{\rho_m})^{-1} \times V_{assay} \qquad \text{Eqn. (3)}$$

where M_{total} is total PM mass collected on the filter, V_e is the original extraction volume (3 mL), $\Delta M_{extract}$ is the change in extract mass due to methanol evaporation by N_2, ρ_m is the density of methanol (0.7918 g/mL), and V_{assay} is the volume of extract added per assay (0.100 mL). All

extracts were covered with aluminum foil to prevent degradation of light-sensitive species and stored in a refrigerator when not in use.

DTT Assay Procedure

The DTT assay was conducted similar to procedures outlined by Cho *et al.* (2005) with additional treatment of the phosphate buffer with Chelex resin (Charrier and Anastasio 2012). Chelex treatment improves assay repeatability by removing trace transition metals from stock buffers and lowering background DTT oxidation (Charrier and Anastasio 2012). The traditional DTT assay measures the oxidation of reduced DTT to its disulfide form over time (Kumagai et al. 2002); an assay schematic is shown in Figure 4. After mixing PM with DTT in solution for a period of time, the remaining, unreacted (reduced) DTT is oxidized by addition of excess Ellman's reagent (5,5'-dithibis-2-nitrobenzoic acid or DTNB). The reaction of DTT with DTNB produces a yellow chromophore (5-mercapto-2-nitrobenzoic acid or TNB), in direct proportion to the amount of reduced DTT remaining in solution. The chromophore is then quantified with UV/VIS spectroscopy and the rate of DTT consumption, ΔDTT is calculated with Eqn. (4):

$$\frac{\Delta DTT}{\Delta t} = \Delta DTT_{sample} - \Delta DTT_{blank} \qquad \text{Eqn. (4)}$$

where ΔDTT_{sample} is the change in DTT amount over time due to oxidation by PM and ΔDTT_{blank} is background DTT oxidation over time measured from a blank sample. For these assays, triplicate 100 µL samples of concentrated PM extract was added to 100 µM DTT in

chelex-treated phosphate buffer at pH 7.4 (600 µL total reaction volume). The reaction mixture was incubated at 37 ºC with 250 µL aliquots removed and quenched in an equal volume of 10% trichloroacetic acid at five minute intervals. The remaining reduced DTT was oxidized by 25 µL of 10 mM DTNB producing the chromophore TNB. This solution was diluted with 500 µL of 0.4 M Tris-HCl buffer, pH 8.9, containing 20 mM EDTA. Absorbance of TNB was measured in triplicate samples at a wavelength of 412 nm.

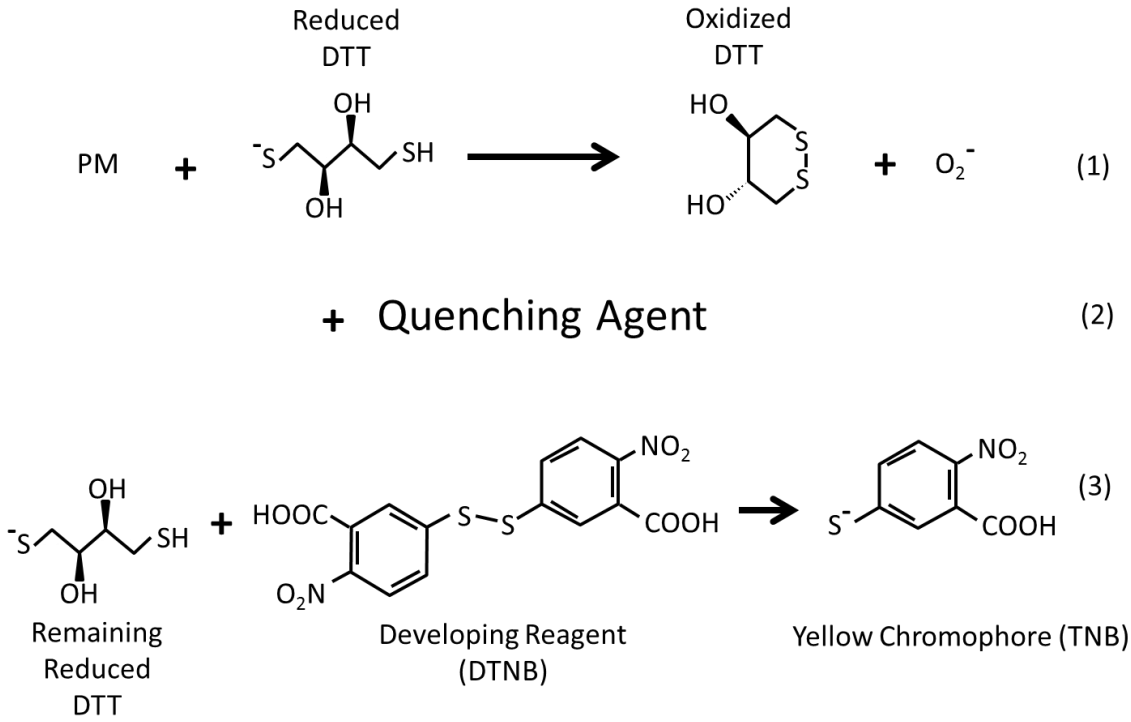

Figure 4: The traditional DTT assay chemical reaction. Electron transfer from DTT to oxygen is catalyzed by PM yielding superoxide anion (O_2^-). A quenching agent stops the reaction and a developing reagent produces a yellow chromophore for absorbance quantification at 412 nm.

For comparison with other studies, urban dust reactivity was reported both in terms of raw DTT consumption rate (DTT amount consumed/minute) and DTT consumption rate normalized by PM mass (μg_{pm}) in the reaction volume. Raw DTT consumption rate was calculated as the linear decline in TNB absorbance over time minus the corresponding decrease

for a similarly treated sample blank. The blank-corrected slope, $\frac{\Delta DTT}{\Delta t}$, was converted to units of DTT amount (nmol) consumed based on a calibration curve of absorbance measurements from stock DTT solutions prepared via serial dilution (Figure 5).

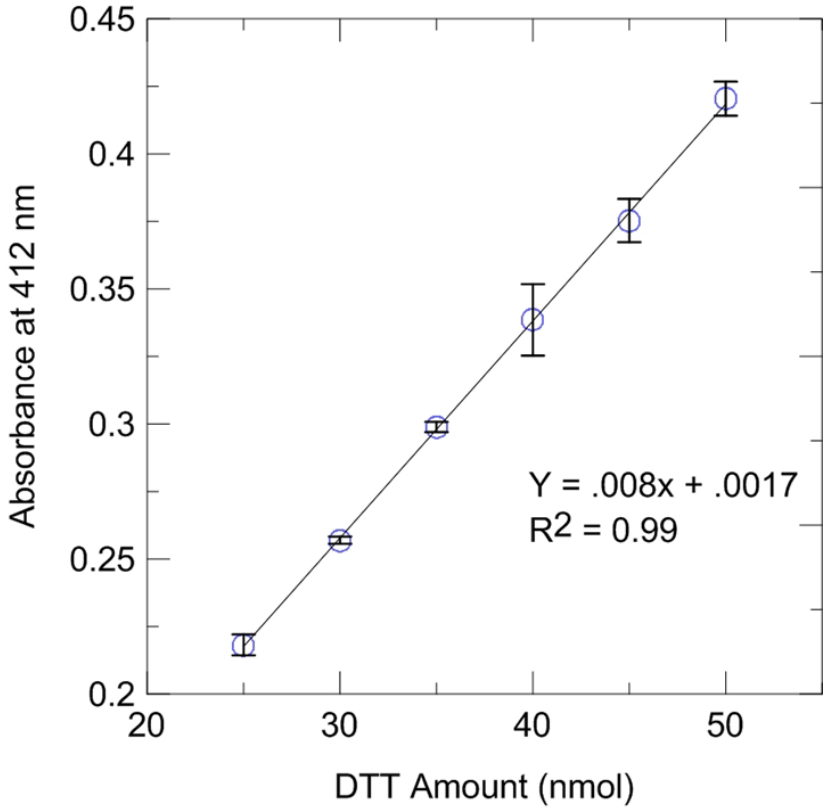

Figure 5: Example calibration curve of relevant DTT amounts and associated spectroscopy absorbance measurements.

Results were considered acceptable if the following measurement criteria were met: (1) the measured rate of DTT consumption fell within the linear range (i.e. 2-25% total DTT consumed); (2) the coefficient of variation was less than 15% among triplicate measures of a given sample (Cho et al. 2005); and (3) the consumption rate of the sample was significantly larger than the blanks using a one-tailed t-test ($\alpha = 0.05$).

On-line DTT Monitoring

System Design

The on-line reactivity monitoring system was designed to collect PM directly into a solution containing DTT, with subsequent continuous measurement of DTT consumption rate using electrochemical detection. Aerosol was collected into solution using a PILS (ADI 2081, Metrohm, Riverview, FL, USA). The PILS, shown in Figure 6, samples ambient PM and immediately mixes the sampled aerosol stream with a turbulent flow of steam (~1.5 mL/min of de-ionized water at 100 °C). The water-saturated aerosol rapidly cools as it travels through the PILS, eventually reaching supersaturation. Particles act as condensation nuclei and grow large enough (aerodynamic diameter, d_{ae} > 1 μm) for collection by impaction onto a plate at the back of the PILS. A reagent solution, introduced above the impaction plate, flows down and carries impacted PM out through a liquid exit below the impaction plate. This continuous flow of PM + reagent solution (aided by a de-bubbler system) is then pumped downstream for on-line chemical analysis.

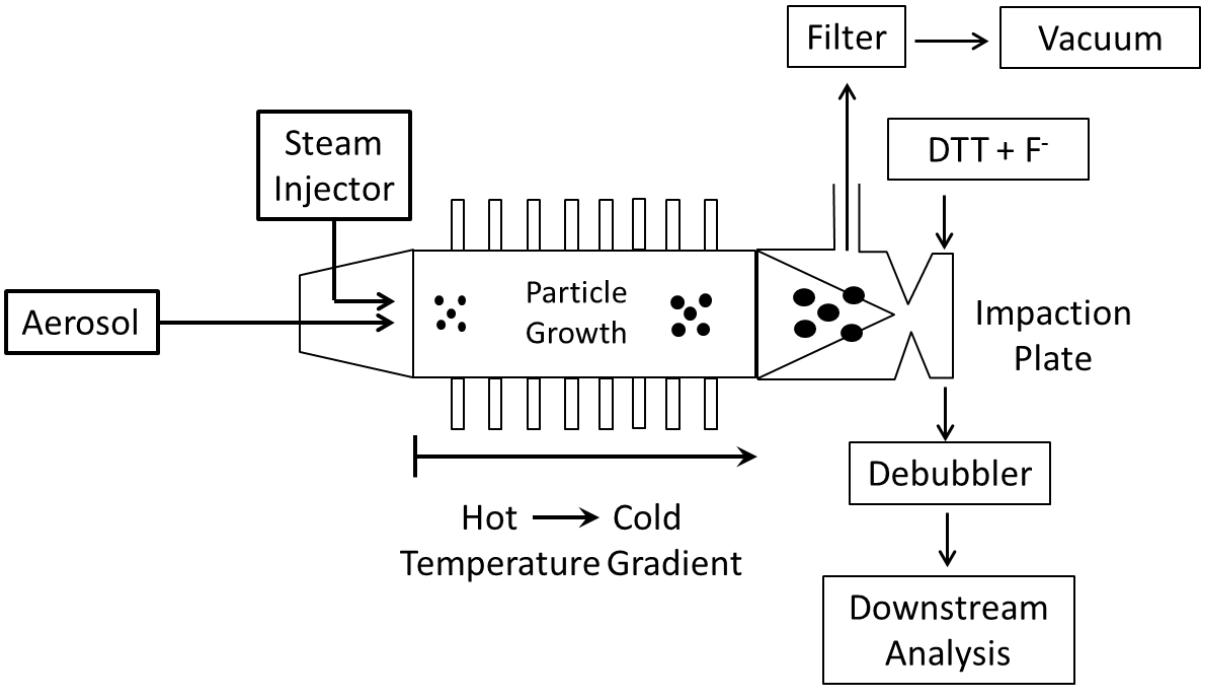

Figure 6: Schematic of the PILS. A PM + steam mixture is cooled creating supersaturated conditions. Particles serve as condensation nuclei and grow into droplets large enough (d_{ae} > 1 µm) for collection at an impaction plate. DTT + F^- enters above the plate and a continuous liquid flow is pumped downstream for electrochemical measurement of DTT consumption.

For on-line PM reactivity monitoring, the buffered reagent solution contained 50 µM of DTT reagent and 100 µM of sodium fluoride (NaF) internal standard. A T-junction integrated with a de-bubbler system immediately split the PM + DTT reaction mixture into equal-volume sample lines. One sample line was collected for ion chromatography (IC) to measure F^- ion/internal standard concentration. The F^- internal standard accounted for DTT dilution due to mixing with PM condensate; lower levels of F^- indicated higher levels of sample dilution. The second sample line was sent to a CoPC microfluidic chip for electrochemical analysis of unreacted (reduced) DTT. All solutions were transported using a multichannel peristaltic pump (Ecoline, IDEX Health and Science, Glattbrug, Switzerland). Tubing lengths and peristaltic

pump speed were adjusted to permit an 18-minute residence time for DTT consumption, as measured from impaction to collection for IC analysis or electrochemical DTT measurement.

On-line Reactivity Measurement

Electrochemical analysis of reduced (unreacted) DTT was controlled by a manual six-way valve for regulated flow injection analysis. Aliquots of 10 µL PM + DTT reaction mixture were injected into the microfluidic sensor at ~three minute intervals. The microfluidic chip was housed inside a Faraday cage to reduce background electrical noise. Electrical conductivity of reduced DTT from each injection was measured via amperometry. As shown in Figure 7, higher amplitude peaks indicated higher levels (i.e., less consumption) of DTT. Therefore, peak height decreases as DTT is consumed by reaction with sampled PM. Peak height was measured and related to DTT mass based on the calibration curve constructed from direct injection of relevant DTT amounts shown in Figure 8.

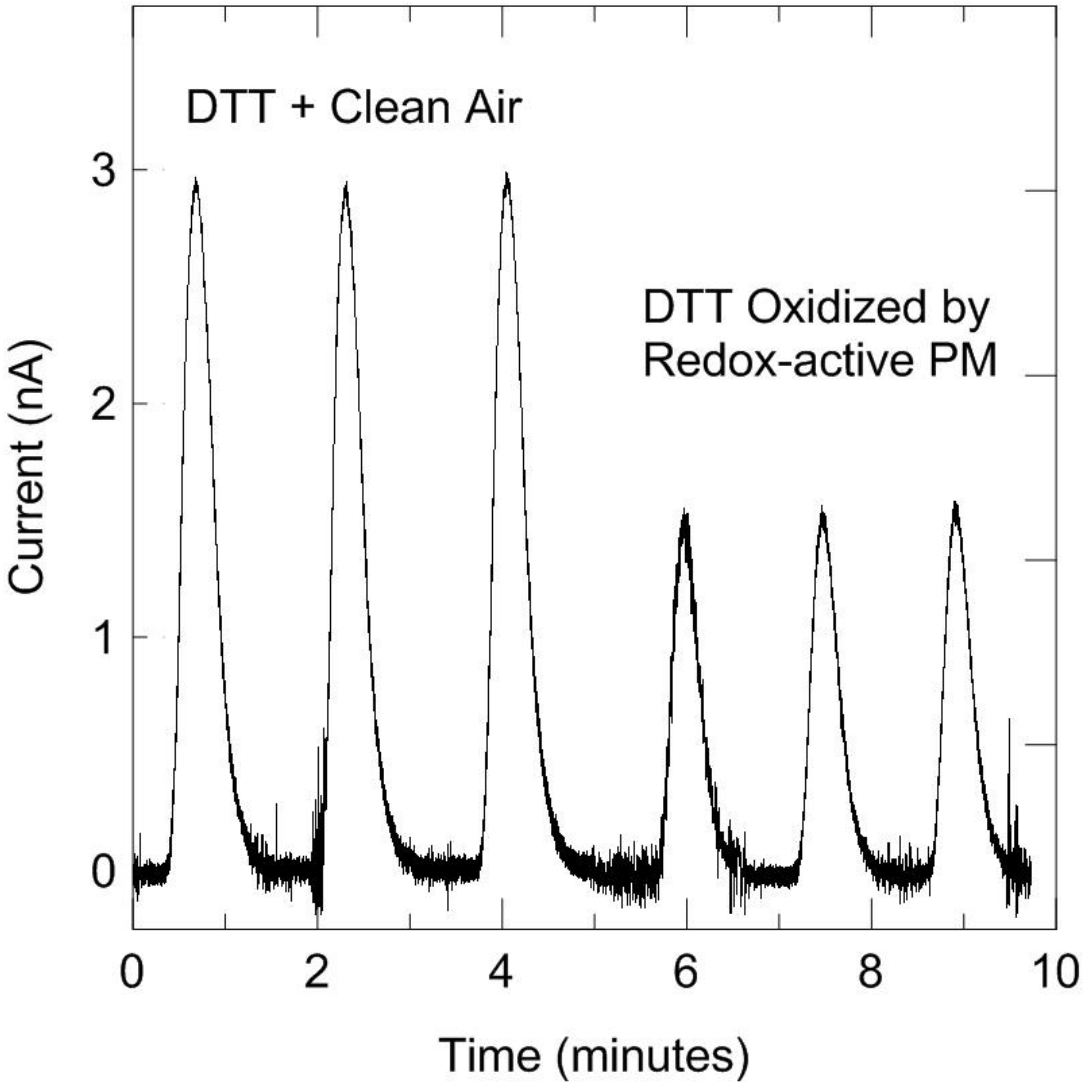

Figure 7: Example time series of DTT signal peaks as detected by the microfluidic sensor. Reduced DTT amount is directly proportional to peak height. Removal of DTT via oxidation by redox-active PM reduces conductivity of the reaction volume. Regular 10 µL injections permit rapid monitoring of changes to ambient PM reactivity.

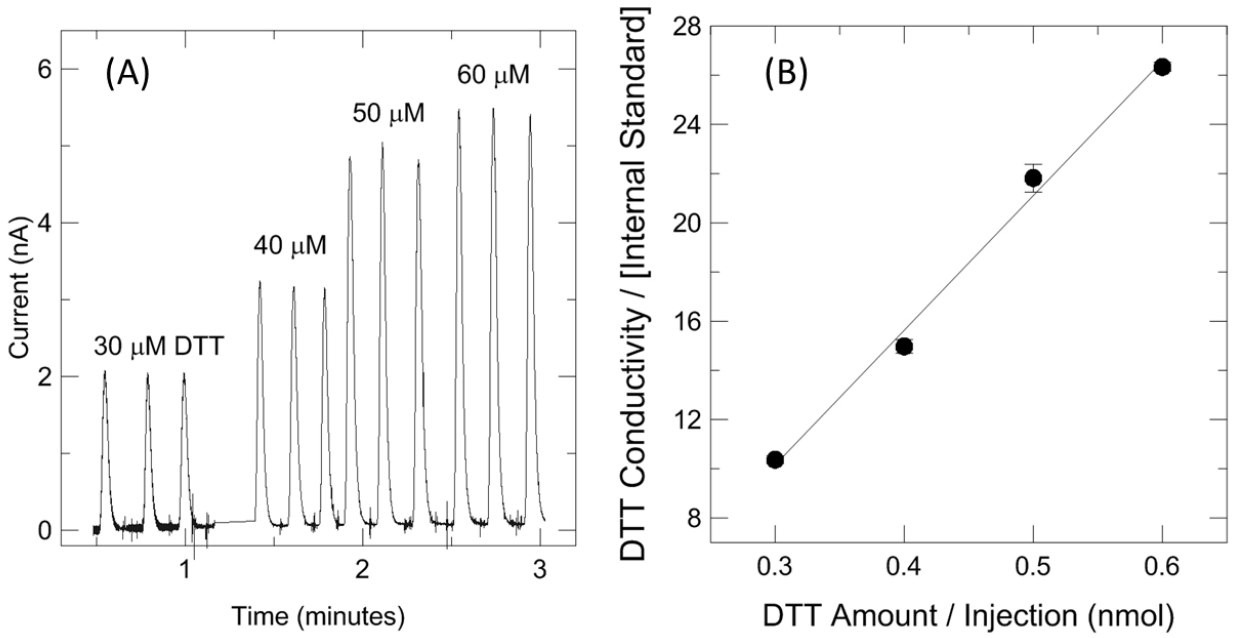

Figure 8: (A) Direct flow injection of relevant reduced DTT amounts. (B) Calibration curve relating conductivity normalized by F^- internal standard concentration.

Raw consumption rate, ΔDTT, was calculated with Eqn. (5):

$$\Delta DTT = \frac{\left[\frac{\sum_{i=1}^{n} S_{blank}}{N}\right] - S_{sample}}{T_{residence}} \qquad \text{Eqn. (5)}$$

where S_{blank} is the DTT signal from injections not containing PM (i.e. HEPA filtered air from the PILS), S_{sample} is DTT signal from injections of the PM + DTT reaction mixture, and $T_{residence}$ is the PM residence time within the system starting at impaction and ending with flow injection. Residence time was designed to be 18 minutes, however two different PILS systems were used during these tests and data analysis revealed a 27 minute residence time in the second PILS system. Blocking by PILS system (see statistical analysis) demonstrated no significant

difference between the two systems for either raw or mass-normalized DTT consumption rate. Mass-normalized DTT consumption rate was calculated by dividing raw DTT consumption rate by PM mass per flow injection. Particle mass per flow injection, $\dot{M}_{injection}$, was calculated with Eqn. (6):

$$\dot{M}_{injection} = \frac{V_i \times Q_{PILS} \times R \times C_i}{q_{in}} \quad \text{Eqn. (6)}$$

where V_i represents the volume per injection (10 µL), Q_{PILS} is the volumetric air flow through the PILS (~13 L/min), R accounts for DTT dilution from PM collection as the ratio of internal standard concentration in the prepared DTT solution and after the DTT + F^- solution reaches the impaction plate, C_i is the ambient PM concentration in the test chamber (µg/m^3) calculated from Eqn. (2), and q_{in} represents the flow rate of DTT+F^- ions through the system (0.18 mL/min). On-line monitoring results were accepted as valid if (1) the signal to noise ratio of DTT peaks was a minimum of 3:1 and (2) sample peaks were significantly lower than clean air peaks using a one-sided t-test ($\alpha = 0.05$).

Statistical Analysis

A 3x2 factorial experiment (high, middle, and low PM concentrations, traditional and on-line DTT monitoring) was conducted to evaluate the two measurement techniques. Chamber PM was collected and analyzed for both the on-line monitoring system and filter-based DTT method in parallel. Three replicates were performed at each concentration level for nine total experiments. All data were stored using Excel 2010 (Microsoft Corp., Seattle, WA, USA) and

statistical analysis performed with SAS 9.2 (SAS Institute Inc., Cary, NC, USA). The linear relationship between raw DTT consumption rate and PM mass for each measurement technique were made using *PROC REG* and *PROC CORR*. Qualitative comparison of these linear strengths were made between methods. Due to differences in the measurement approaches (DTT mass by electrochemical detection vs. DTT consumption rate by spectrophotometry), direct comparison of the two methods was made only in terms of mass-normalized DTT consumption rate. Mass-normalized reactivity was modeled as a function of chamber concentration level (high, middle, and low) and DTT measurement approach using *PROC MIXED*. The mixed model was constructed using a *random* statement to account for repeated measures at each injection mass by the on-line system and unbalanced data. An *lsmeans* statement was used to make pairwise comparisons between the on-line and traditional techniques at each concentration level.

Results

Aerosolized Urban Dust and Raw DTT Consumption Rates

The size distribution of aerosolized urban dust was similar across all concentration levels. Urban dust size distribution, shown in Figure 9, was approximately log-normal with count median diameter (CMD) of 41.9 nm and geometric standard deviation of ± 2.1

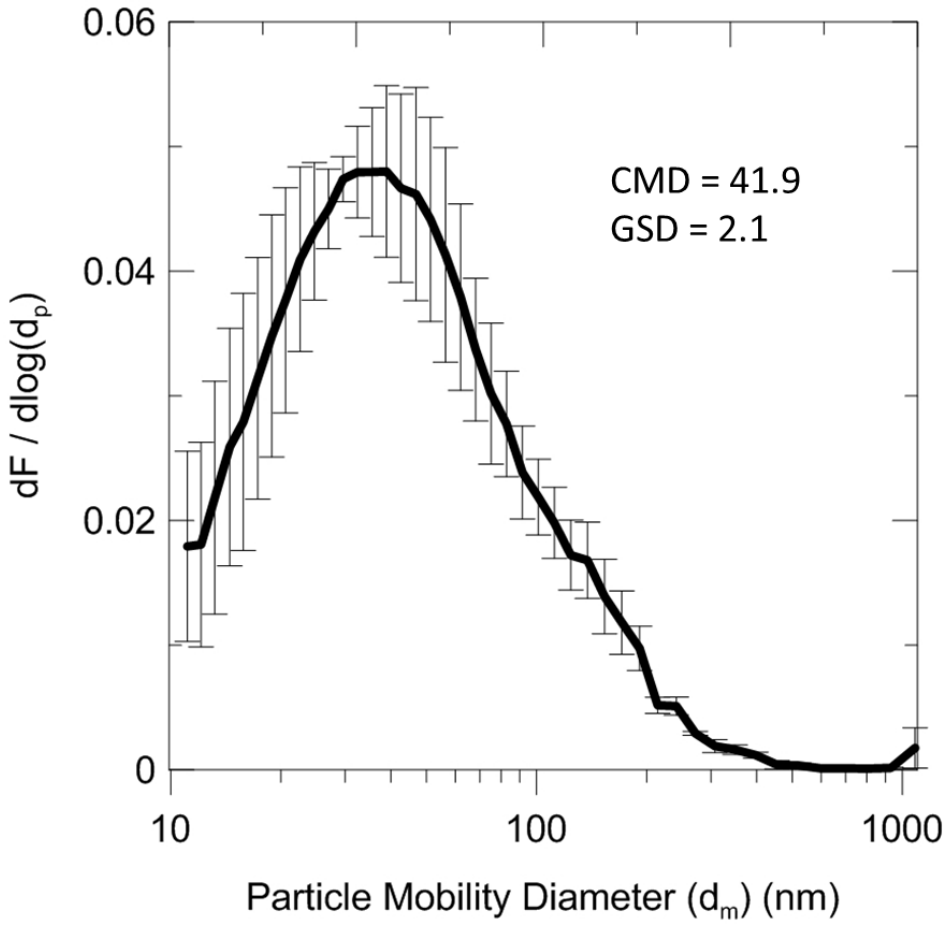

Figure 9: Aerosolized urban dust size distribution (count fraction) averaged over three test replicates; one from each concentration level (high, middle, low).

An example time series plot tracking chamber mass concentration, C_i, from each concentration level is shown in Figure 10.

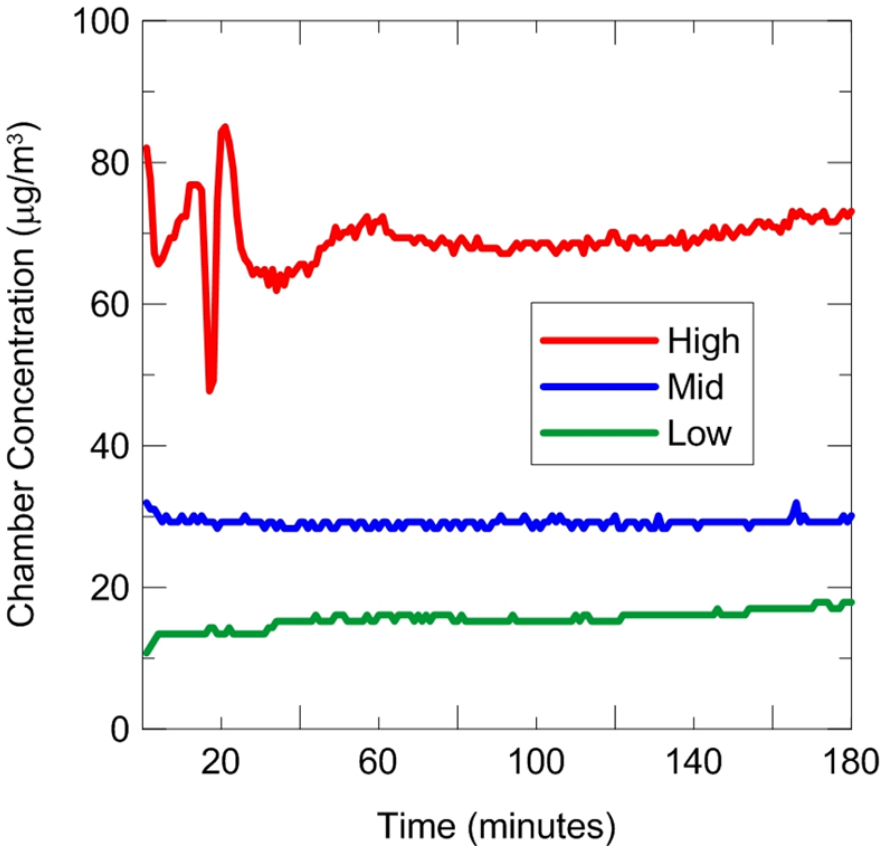

Figure 10: Time series plot showing changes in aerosolized urban dust mass concentration. A representative experimental replicate from each concentration level is shown.

Raw DTT consumption rates estimated by both DTT analysis techniques, as a function of chamber mass, C_i, are shown in Figure 11. The on-line system measured raw DTT consumption rates that correlated strongly with chamber concentration (R^2 = 0.91, p < 0.0001) and an intercept near zero (b = 0.19 pmol DTT, p = 0.43). Raw DTT consumption rates measured by the traditional method were also significantly correlated with chamber concentration, but with more variability than the on-line system (R^2 = 0.69, p < 0.0001) and a non-zero intercept (b = 160.6 pmol DTT, p < 0.0001).

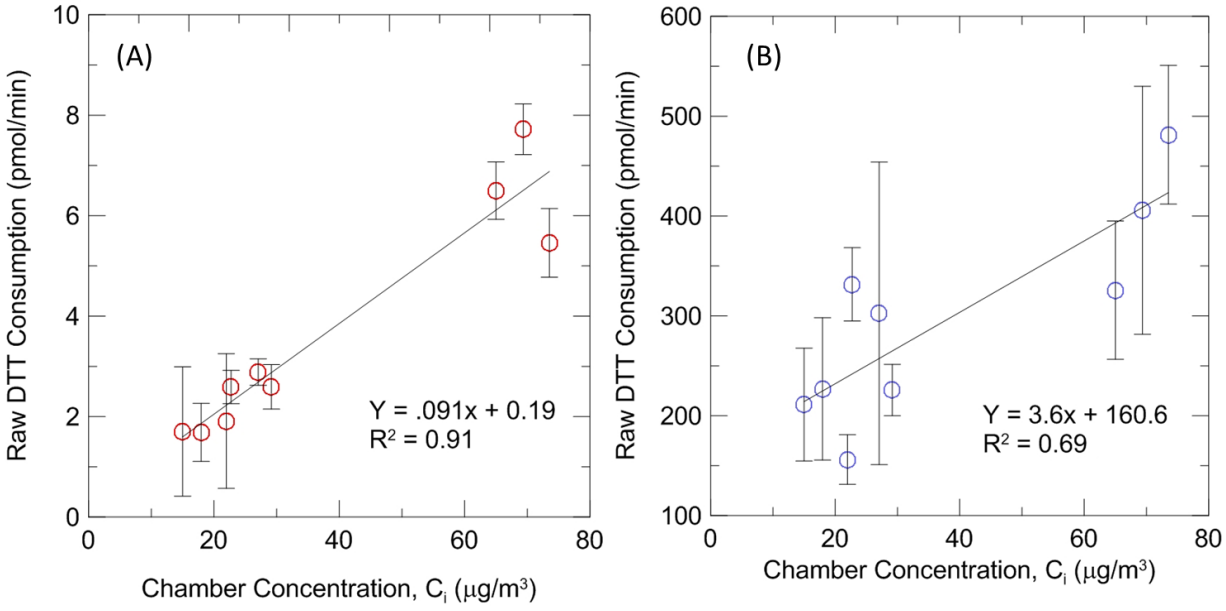

Figure 11: Correlation diagrams of raw DTT consumption versus corrected chamber mass measured by (A) On-line and (B) Traditional DTT monitoring. Estimates for slope, intercept, and Pearson correlation coefficients are shown for each plot.

Raw DTT consumption rates detected by both DTT analysis techniques, as a function of PM mass per injection, $\dot{M}_{injection}$, or mass per assay, M_{assay}, are shown in Figure 12. Raw DTT consumption rates measured by the on-line system strongly correlated with mass per injection $\dot{M}_{injection}$ (R^2 = 0.93, p < 0.0001) with a small, but statistically significant intercept (b = 0.52

pmol DTT, p = 0.011). Alternatively, the traditional DTT method did not detect a significant linear relationship between raw DTT consumption rate and PM mass per assay (R^2 = 0.29, p = 0.15). Stronger correlations were observed with the on-line system from analysis of significantly smaller PM mass quantities than by the traditional method. Sample mass per on-line injection, $\dot{M}_{injection}$, averaged 34 ± 22 ng (one standard deviation) and ranged from 11 to 68 ng. Concentrated PM mass per traditional assay, M_{assay}, was nearly three orders of magnitude larger and averaged 4.4 ± 2.2 µg and ranged from 1.9 to 9.6 µg.

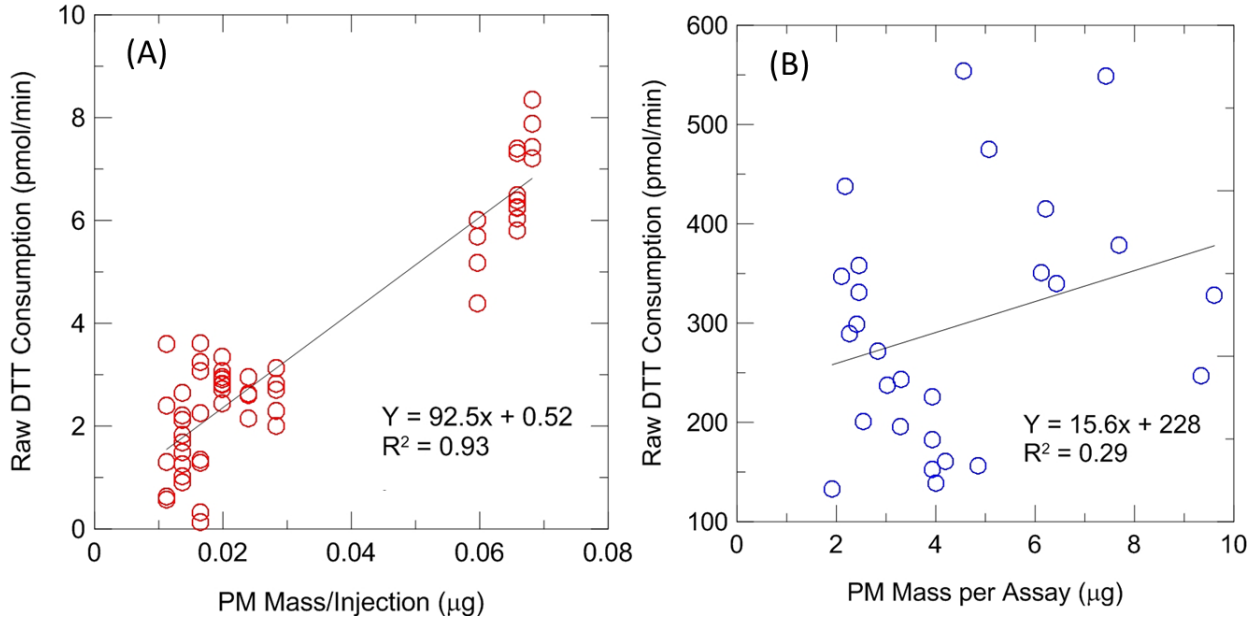

Figure 12: Correlation diagrams of raw DTT consumption versus PM mass within individual assays. Estimates for slope, intercept, and Pearson correlation coefficients are shown for (A) On-line detection of raw DTT consumption versus $\dot{M}_{injection}$, PM mass per injection and (B) Traditional measurement of raw DTT consumption versus M_{assay}, PM mass per assay.

Mass-Normalized DTT Consumption Rate

Box-whisker plots comparing mass-normalized DTT consumption rates by each technique versus chamber concentration as a categorical variable are shown in Figure 13. The

boxplots show median, quartile, and 95% confidence limits of the mean DTT consumption rate for each chamber concentration level. Mass-normalization of on-line measurements by $\dot{M}_{injection}$ showed no significant difference between concentration levels. The on-line system gave an average, characteristic DTT consumption rate of 115.7 ± 6.2 pmol DTT/min/μg_{pm} for urban dust (SRM 1649b). Mass-normalization of filter-based DTT analysis by M_{assay} also demonstrated no significant difference between concentration levels. However, traditional tests at mid-level concentrations were marginally non-significant from low ($p = .068$) and high ($p = .066$) concentration tests. The traditional method gave an average, characteristic DTT consumption rate of 80.7 ± 8.6 pmol DTT/min/μg_{pm} for urban dust, an ~40% lower estimate.

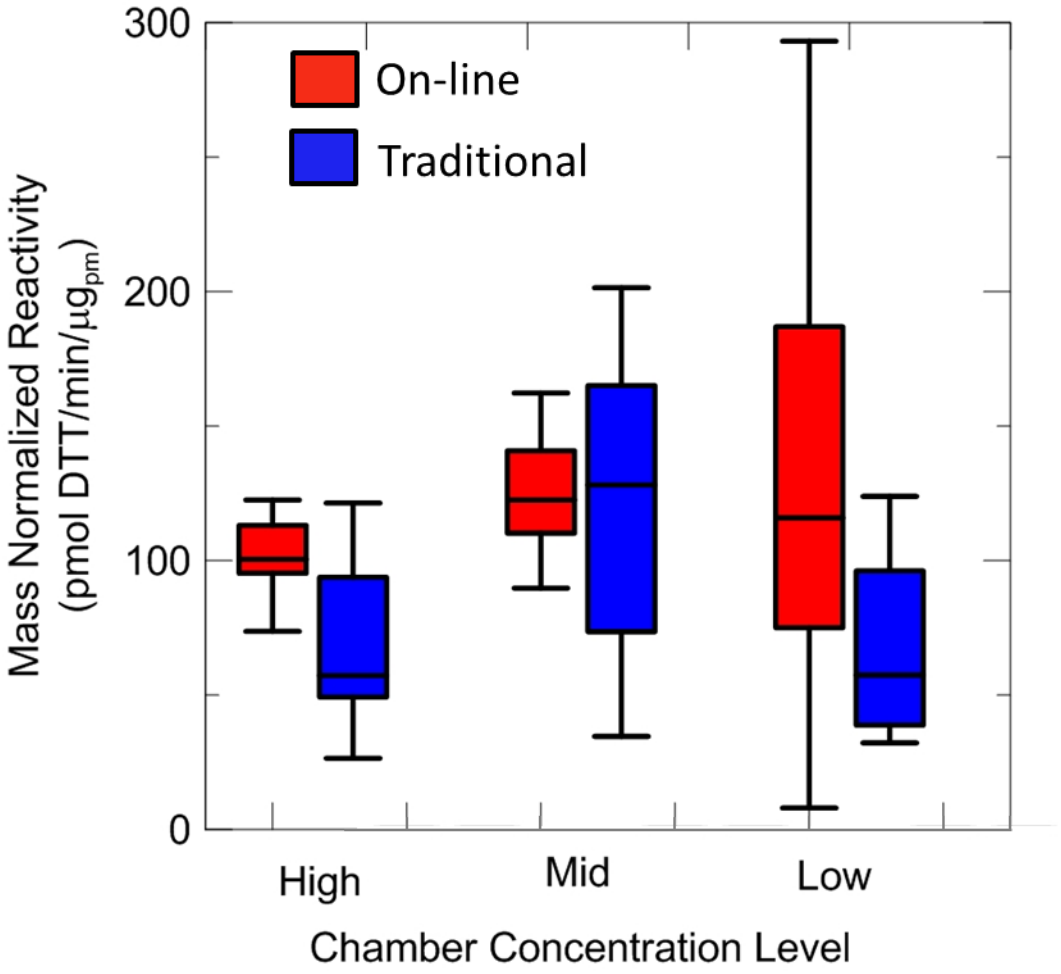

Figure 13: Box-whisker plots of mass-normalized DTT reactivity measured by each monitoring approach as a function of chamber concentration level.

When stratified by chamber concentration, the on-line system reported higher mass-normalized DTT consumption rates than the traditional method (Table 1). The on-line monitoring system measured higher average mass-normalized reactivity values at all concentration levels. Two-tailed testing of differences between DTT approaches were significant at low chamber concentrations ($p = 0.037$), non-significant at middle concentrations ($p = 0.57$), and marginally non-significant at high ($p = 0.0926$).

Table 1: Mixed Model Analysis Results

Concentration Level	**Method**	**Reactivity (pmol DTT/min/μg_{pm})**	**P-value***
High	On-line	102.9 ± 11.3	0.093
	Traditional	64 ± 14.9	
Middle	On-line	124.9 ± 10.9	0.57
	Traditional	113.5 ± 14.9	
Low	On-line	119.3 ± 12.5	0.037
	Traditional	64.7 ± 14.9	
Combined	On-line	115.7 ± 6.2	0.022
	Traditional	80.7 ± 8.6	

Pairwise comparisons of mass-normalized DTT consumption rate estimates for each method, separated by concentration level. Statistical comparisons of estimates were performed with mixed-model analysis using concentration level and DTT method to predict mass-normalized reactivity. *P-values were estimated with two-tailed t-tests of difference in means.

Discussion

This study demonstrated the utility of the on-line monitoring approach for aerosol reactivity and the flaws associated with the traditional DTT approach. The on-line monitoring system exhibited improved performance as demonstrated by multiple metrics. A stronger linear correlation was observed between raw DTT consumption rate and PM mass (both in the chamber and reaction volume) by the on-line system compared to the traditional assay. Further, the on-line system reported an intercept near-zero for a regression of chamber mass versus raw reactivity in contrast with the traditional assay which reported a significantly non-zero intercept. A non-zero intercept implies the presence of a systematic bias between assayed PM mass and aerosol reactivity (Senn et al. 2000). For mass-normalized data, on-line measurements were more precise (i.e. less variable) than corresponding traditional measures at all concentration levels and most experimental replicates (± 6.2 overall SE on-line versus ± 8.6 SE traditional). However, variability of the on-line measurements increased as PM mass decreased, suggesting that a 10 $\mu g/m^3$ concentration is near the limit of detection (LOD) for this technique. For DTT analysis, LOD is defined as the minimum sample mass required to generate a signal distinguishable from a blank. The ratio of sample to blank DTT measurements by each method for all experimental replicates is shown in Figure 14. For on-line monitoring, slight overlap between distributions of sample and blank DTT amounts (error bar crossing y = 1) was observed at the lowest concentration test indicating nearness to the LOD. Sample dilution by the on-line system occurs due to steam condensation from the PILS and buffered DTT flow across the impaction plate. The on-line system LOD may be lowered by reducing these flows to permit more concentrated PM in the sample lines. This may be practical for low ambient concentrations (<10 $\mu g/m^3$) at the cost

of reduced temporal resolution. Sampling with open-faced filter cassettes at an increased flow of 20 L/min combined with concentrating PM extracts by evaporation permitted traditional analysis to avoid LOD at lower ambient concentrations.

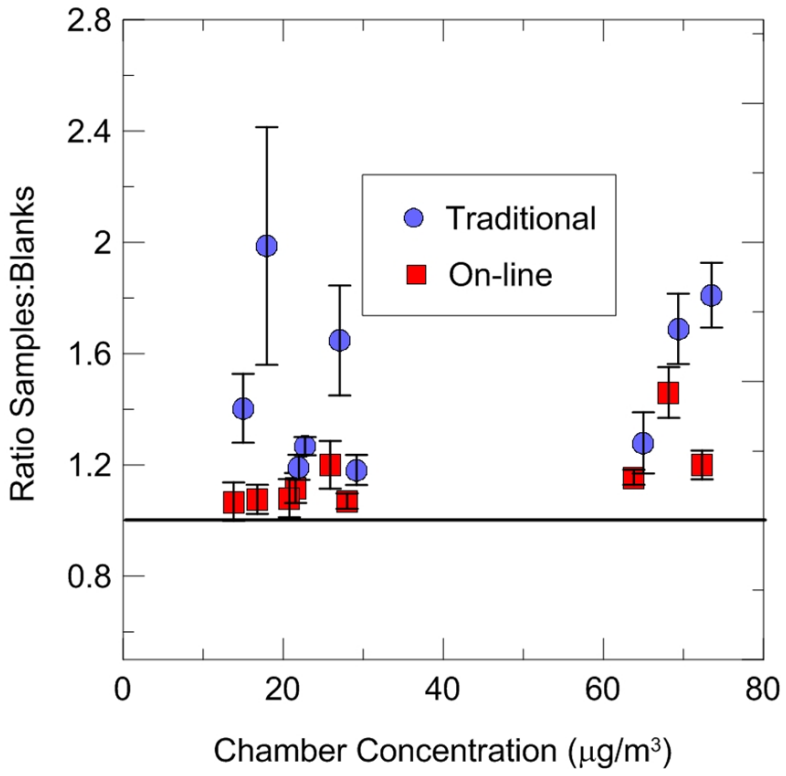

Figure 14: Scatterplot showing ratios of DTT amount measured by urban dust and blank samples. Ratios approaching unity suggest measurements approaching the limit of detection.

Injection masses measured by the on-line system ranged from between 76 and 375 times less than corresponding traditional readings. Reaction volume was reduced to 10 µL opposed to 600 µL we used for traditional analysis and even more dilute 3 mL reaction volume reported by many others (Charrier and Anastasio 2012; Cho et al. 2005; Li et al. 2009a; Rattanavaraha et al. 2011). On-line monitoring permitted near-continuous analysis of PM reactivity. Electrochemical injections were measured at ~three minute intervals while each traditional DTT measurement described a three-hour filter sample. Additionally, PM mass per injection for on-line readings

correlated with chamber concentration, C_g, (R^2 = 0.98) more strongly than PM mass per traditional measurement correlated with C_g, (R^2 = 0.79). This indicates on-line measurements of DTT consumption rate better reflected ambient conditions than off-line analysis of filter extracts.

A combination of random and biased estimates of PM mass in sample extracts may explain poor raw and mass-normalized DTT consumption rates detected by traditional analysis. Traditional filter handling, extraction, and concentration protocols presented numerous chances for redox-active PM losses, thus systematically inflating estimates of PM mass per assay. Filter samples were processed individually; therefore the magnitude of loss was random. Estimates of raw DTT consumption rates of traditional sample extracts may have been accurate; however correlation with uncertain PM masses would weaken linear strength suggesting assay variability due to random error. Division by systematically overestimated PM mass per assay likely lowered mass-normalized reactivity values while the random errors resulted in greater standard error estimates from the mass-normalized traditional data. In comparison, the PILS collection method endured fewer PM losses as demonstrated by stronger correlations between reactivity and PM mass and consistently higher mass-normalized reactivity estimates. Solutions were transported inside sealed tubing with no environmental exposure prior to electrochemical DTT measurement which eliminated evaporative losses. The on-line system also employed a DTT dilution factor using the internal standard (F^-) providing more confident estimates of PM mass per injection. Applying an internal standard to traditional filter extracts may improve PM mass per assay estimates. Finally, increased mass-normalized DTT consumption rate estimates by the on-line system may be influenced by trace metals present within on-line sampling lines whereas traditional assay buffers were chelex-treated.

Charrier and Anastasio (2012) reported non-linear raw DTT consumption response to PM mass from the traditional assay and attributed the phenomenon to high metal concentrations. Certain metals (most notably copper) are known to alter reduced DTT by the formation of binding complexes in addition to oxidation (Kachur 1997; Krezel et al. 2001). Charrier and Anastasio (2012) experimentally observed this phenomenon to occur when Cu(II) and Mn(II) are present at or above a 1:1 molar ratio with DTT. However, small reported mass fractions of transition metals in SRM 1649b suggest DTT binding did not impact the results reported here. Copper constitutes only 0.14 µg/mg of urban dust, Zn composition is 1.48 µg/mg, and total metals are 8.42 µg/mg (Costa and Dreher 1997). Mass ratios of DTT to *total* PM per measurement observed from our study are shown in Figure 15. Ratios ranged from 1:1 at high chamber concentrations to 7:1 for low concentration tests suggesting high metal concentrations were not an issue. Additionally, the on-line system measured PM reactivity from DTT:PM mass ratios comparable with the traditional method. If DTT binding caused non-linearity the same phenomenon may have also impaired on-line reactivity measurements.

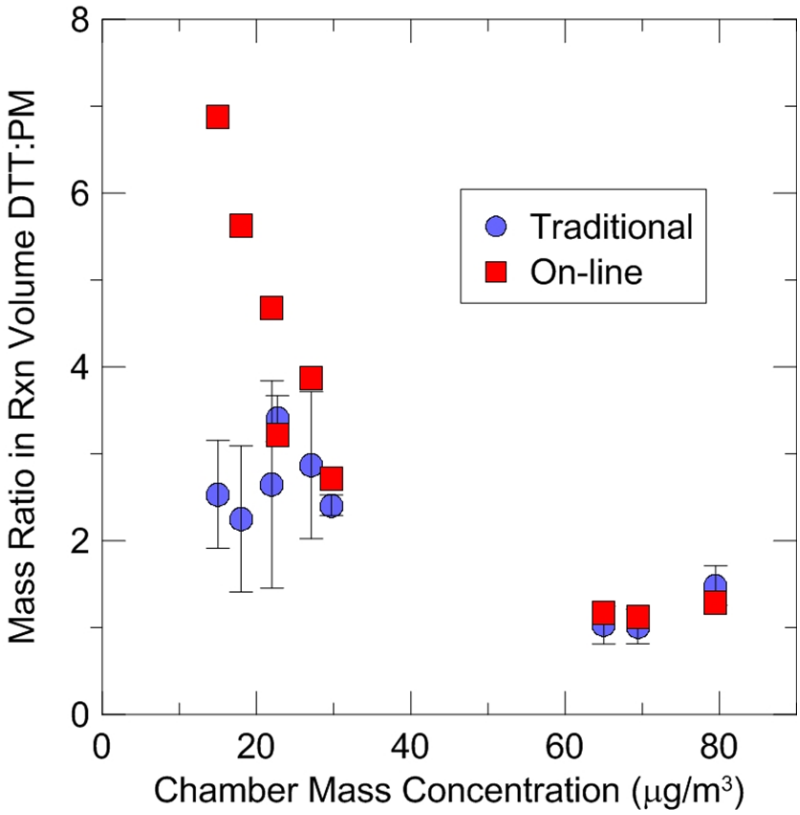

Figure 15: Correlation diagram comparing ratios between DTT and PM mass for each experimental replicate. Data from the on-line system lack error bars because one mass value was applied to all injections in each experimental replicate.

Despite significant advances in PM reactivity monitoring demonstrated by the on-line system, certain limitations warrant attention. The PILS requires ultra-pure DI water to collect PM, therefore only water-soluble PM fractions are collected for DTT analysis. However, the methanol-soluble fraction of urban dust was more reactive than the water-soluble fraction (Figure 3). Mixing small volumes of methanol or other solvents downstream of the impaction plate may permit higher efficiency capture of redox-active species. Regardless of this limitation, the on-line system detected ~1.4 times greater mass-normalized reactivity of aerosolized urban dust than the traditional method. These data suggest volatile or highly reactive species captured by the PILS were present within the sample line to consume DTT. Mixing additional solvents

downstream of the impaction plate may permit higher efficiency capture and measurement of redox-active PM. Another drawback to the on-line system is less-than-desirable portability in the current configuration. Despite the microfluidic chip's small size, ancillary equipment such as the potentiostat, air pump, peristaltic pump, and Faraday cage are bulky and/or heavy. Recent product advances, such as pocket-sized potentiostats, offer improvement. Secondary equipment is also sensitive to outside perturbations requiring installation of protective devices and thorough evaluation of sampling locations. For example, peristaltic pump tubing is soft and easily disturbed, the PILS must sit at a 15° angle for efficient particle collection, and the potentiostat is capable of detecting background electrical fields that may interfere with electrochemical measurements.

Conclusions

This study represents a formal evaluation of a new approach for assessing PM reactivity. A PILS was coupled with a CoPC-microfluidic chip to permit continuous, on-line measurement of DTT consumption by PM. The on-line system outperformed traditional techniques in laboratory analysis of standardized urban dust in several regards. The on-line system more strongly correlated raw DTT consumption rate with PM mass and detected greater characteristic mass-normalized DTT consumption than the traditional approach. On-line data were less variable than corresponding traditional measures for both raw and normalized DTT consumption measures. The on-line system improved DTT monitoring from reduced sample quantities, reaction volumes, and PM handling time compared to the traditional technique. These results suggest on-line monitoring for DTT reactivity may provide an improved tool for researchers investigating the impact of PM on human health.

Future Work

The on-line monitoring system should be further refined in a laboratory setting prior to field deployment. Neither a limit of detection nor a limit of quantification of aerosolized urban dust mass has been formally evaluated. An experiment investigating electrochemical response to decreasing PM mass will reveal these parameters. The impact of using chelex-treated buffer used by the on-line system should be investigated as well. Chelex-treatment significantly reduces variability of the traditional DTT assay. Similar reductions in variability for electrochemical DTT sensing would further lower PM mass requirements. Another study should assess the effect of mixing additional extraction solvents downstream of the PILS impaction plate. The current on-line system captures only the water-soluble fraction of urban dust which was observed to be less DTT reactive than the methanol-soluble fraction (Figure 3). Supplementary extraction solvents may provide more DTT analysis of a more comprehensive fraction of redox-active PM. Assessing the practicality of multiplexed CoPC-microfluidic chips for immediate sensing of internal standard concentration should also be investigated. This improvement would eliminate split sample lines and off-line IC analysis while concentrating PM in the sample line thus lowering LOD. Finally, reconfiguration of the on-line system should be performed prior to field deployment. Installation of protective coverings for sensitive peristaltic pump tubing and obtaining more portable ancillary equipment (i.e. smaller potentiostat, Faraday cage, and air pump) will make the system more amenable for field investigations.

References

Alessandrini F, Beck-Speier I, Krappmann D, Weichenmeier I, Takenaka S, Karg E, et al. 2009. Role of Oxidative Stress in Ultrafine Particle–induced Exacerbation of Allergic Lung Inflammation. American Journal of Respiratory and Critical Care Medicine 179:984 – 991; doi:10.1164/rccm.200807-1061OC.

Aust AE, Ball JC, Hu AA, Lighty JS, Smith KR, Straccia AM, et al. 2002. Particle characteristics responsible for effects on human lung epithelial cells. Res Rep Health Eff Inst 1–65; discussion 67–76.

Bateman AP, Nizkorodov SA, Laskin J, Laskin A. 2010. High-Resolution Electrospray Ionization Mass Spectrometry Analysis of Water-Soluble Organic Aerosols Collected with a Particle into Liquid Sampler†. Anal. Chem. 82:8010–8016; doi:10.1021/ac1014386.

Becher R, Bucht A, Øvrevik J, Hongslo JK, Dahlman HJ, Samuelsen JT, et al. 2007. Involvement of NADPH Oxidase and iNOS in Rodent Pulmonary Cytokine Responses to Urban Air and Mineral Particles. Inhalation Toxicology 19:645–655; doi:10.1080/08958370701353528.

Beer D, Weber J. 1972. Photobleaching of organic laser dyes. Optics Communications 5:307–309; doi:10.1016/0030-4018(72)90105-8.

Bernardoni V, Cuccia E, Calzolai G, Chiari M, Lucarelli F, Massabò D, et al. 2011. ED-XRF set-up for size-segregated aerosol samples analysis. X-Ray Spectrometry 40:79–87; doi:10.1002/xrs.1299.

Brook RD, Rajagopalan S, Pope CA, Brook JR, Bhatnagar A, Diez-Roux AV, et al. 2010. Particulate Matter Air Pollution and Cardiovascular Disease: An Update to the Scientific Statement From the American Heart Association. Circulation 121:2331–2378; doi:10.1161/CIR.0b013e3181dbece1.

Chahine T, Baccarelli A, Litonjua A, Wright RO, Suh H, Gold DR, et al. 2007. Particulate air pollution, oxidative stress genes, and heart rate variability in an elderly cohort. Environ. Health Perspect. 115:1617–1622; doi:10.1289/ehp.10318.

Charrier JG, Anastasio C. 2012. On dithiothreitol (DTT) as a measure of oxidative potential for ambient particles: evidence for the importance of soluble transition metals. Atmospheric Chemistry and Physics Discussions 12:11317–11350; doi:10.5194/acpd-12-11317-2012.

Cho AK, Sioutas C, Miguel AH, Kumagai Y, Schmitz DA, Singh M, et al. 2005. Redox activity of airborne particulate matter at different sites in the Los Angeles Basin. Environmental Research 99: 40–47.

Chung MY, Lazaro RA, Lim D, Jackson J, Lyon J, Rendulic D, et al. 2006. Aerosol-borne quinones and reactive oxygen species generation by particulate matter extracts. Environmental science & technology 40: 4880–4886.

Costa DL, Dreher KL. 1997. Bioavailable transition metals in particulate matter mediate cardiopulmonary injury in healthy and compromised animal models. Environ Health Perspect 105: 1053–1060.

Dockery DW, Pope CA 3rd, Xu X, Spengler JD, Ware JH, Fay ME, et al. 1993. An association between air pollution and mortality in six U.S. cities. N. Engl. J. Med. 329:1753–1759; doi:10.1056/NEJM199312093292401.

Eeden SF van, Tan WC, Suwa T, Mukae H, Terashima T, Fujii T, et al. 2001. Cytokines involved in the systemic inflammatory response induced by exposure to particulate matter air pollutants (PM(10)). Am. J. Respir. Crit. Care Med. 164: 826–830.

Fine PM, Shen S, Sioutas C. 2004. Inferring the Sources of Fine and Ultrafine Particulate Matter at Downwind Receptor Sites in the Los Angeles Basin Using Multiple Continuous Measurements Special Issue of Aerosol Science and Technology on Findings from the Fine Particulate Matter Supersites Program. Aerosol Science and Technology 38:182–195; doi:10.1080/02786820390229499.

Foucaud L, Wilson M, Brown D, Stone V. 2007. Measurement of reactive species production by nanoparticles prepared in biologically relevant media. Toxicology letters 174: 1–9.

Fujii T, Hayashi S, Hogg JC, Mukae H, Suwa T, Goto Y, et al. 2002. Interaction of Alveolar Macrophages and Airway Epithelial Cells Following Exposure to Particulate Matter Produces Mediators That Stimulate the Bone Marrow. Am. J. Respir. Cell Mol. Biol. 27: 34–41.

Garcia CD, Henry CS. 2004. Enhanced determination of glucose by microchip electrophoresis with pulsed amperometric detection. Analytica Chimica Acta 508:1–9; doi:10.1016/j.aca.2003.11.060.

Ghelfi E, Rhoden CR, Wellenius GA, Lawrence J, Gonzalez-Flecha B. 2008. Cardiac Oxidative Stress and Electrophysiological Changes in Rats Exposed to Concentrated Ambient Particles are Mediated by TRP-Dependent Pulmonary Reflexes. Toxicological Sciences 102:328 –336; doi:10.1093/toxsci/kfn005.

Hu S, Polidori A, Arhami M, Shafer M, Schauer J, Cho A, et al. 2008. Redox activity and chemical speciation of size fractioned PM in the communities of the Los Angeles? Long Beach Harbor. Atmospheric Chemistry and Physics Discussions 8: 11643–11672.

Ichoku C, Andreae MO, Andreae TW, Meixner FX, Schebeske G, Formenti P, et al. 1999. Interrelationships between aerosol characteristics and light scattering during late winter in an Eastern Mediterranean arid environment. Journal of Geophysical Research 104:24371–24393; doi:10.1029/1999JD900781.

Jokerst JC, Emory JM, Henry CS. Advances in microfluidics for environmental analysis. Analyst 137:24–34; doi:10.1039/C1AN15368D.

Kachur A. 1997. JSTOR: Radiation Research, Vol. 147, No. 4 (Apr., 1997), pp. 409-415. Available: http://0-www.jstor.org.catalog.library.colostate.edu/openurl?volume=147&date=1997&spage=409&issn=00337587&issue=4 [accessed 3 May 2012].

Kim S, Shen S, Sioutas C. 2002. Size distribution and diurnal and seasonal trends of ultrafine particles in source and receptor sites of the Los Angeles basin. J Air Waste Manag Assoc 52: 297–307.

Krezel A, Lesniak W, Jezowska-Bojczuk M, Mlynarz P, Brasuñ J, Kozlowski H, et al. 2001. Coordination of heavy metals by dithiothreitol, a commonly used thiol group protectant. J. Inorg. Biochem. 84: 77–88.

Kumagai Y, Arimoto T, Shinyashiki M, Shimojo N, Nakai Y, Yoshikawa T, et al. 1997. Generation of Reactive Oxygen Species during Interaction of Diesel Exhaust Particle Components with NADPH-Cytochrome p450 Reductase and Involvement of the Bioactivation in the DNA Damage. Free Radical Biology and Medicine 22:479–487; doi:10.1016/S0891-5849(96)00341-3.

Kumagai Y, Koide S, Taguchi K, Endo A, Nakai Y, Yoshikawa T, et al. 2002. Oxidation of Proximal Protein Sulfhydryls by Phenanthraquinone, a Component of Diesel Exhaust Particles. Chemical Research in Toxicology 15:483–489; doi:10.1021/tx0100993.

Li N, Hao M, Phalen RF, Hinds WC, Nel AE. 2003a. Particulate air pollutants and asthma:: A paradigm for the role of oxidative stress in PM-induced adverse health effects. Clinical Immunology 109: 250–265.

Li N, Kim S, Wang M, Froines J, Sioutas C, Nel A. 2002. Use of a stratified oxidative stress model to study the biological effects of ambient concentrated and diesel exhaust particulate matter. Inhal Toxicol 14:459–486; doi:10.1080/089583701753678571.

Li N, Sioutas C, Cho A, Schmitz D, Misra C, Sempf J, et al. 2003b. Ultrafine particulate pollutants induce oxidative stress and mitochondrial damage. Environ Health Perspect 111: 455–460.

Li N, Wang M, Bramble LA, Schmitz DA, Schauer JJ, Sioutas C, et al. 2009a. The Adjuvant Effect of Ambient Particulate Matter Is Closely Reflected by the Particulate Oxidant Potential. Environ Health Perspect 117:1116–1123; doi:10.1289/ehp.0800319.

Li Q, Wyatt A, Kamens RM. 2009b. Oxidant generation and toxicity enhancement of aged-diesel exhaust. Atmospheric Environment 43: 1037–1042.

Mauderly JL, Chow JC. 2008. Health Effects of Organic Aerosols. Inhalation Toxicology 20:257–288; doi:10.1080/08958370701866008.

Mutlu GM, Green D, Bellmeyer A, Baker CM, Burgess Z, Rajamannan N, et al. 2007. Ambient particulate matter accelerates coagulation via an IL-6–dependent pathway. Journal of Clinical Investigation 117:2952–2961; doi:10.1172/JCI30639.

Nemmar A, Hoet PHM, Vanquickenborne B, Dinsdale D, Thomeer M, Hoylaerts MF, et al. 2002. Passage of Inhaled Particles Into the Blood Circulation in Humans. Circulation 105:411–414; doi:10.1161/hc0402.104118.

Noblitt SD, Lewis GS, Liu Y, Hering SV, Collett JL, Henry CS. 2009. Interfacing Microchip Electrophoresis to a Growth Tube Particle Collector for Semicontinuous Monitoring of Aerosol Composition. Anal. Chem. 81:10029–10037; doi:10.1021/ac901903m.

Ntziachristos L, Froines JR, Cho AK, Sioutas C. 2007. Relationship between redox activity and chemical speciation of size-fractionated particulate matter. Particle and Fibre Toxicology 4:5; doi:10.1186/1743-8977-4-5.

Nurkiewicz TR, Porter DW, Barger M, Millecchia L, Rao KMK, Marvar PJ, et al. 2006. Systemic Microvascular Dysfunction and Inflammation after Pulmonary Particulate Matter Exposure. Environ Health Perspect 114:412–419; doi:10.1289/ehp.8413.

Orsini DA, Ma Y, Sullivan A, Sierau B, Baumann K, Weber RJ. 2003. Refinements to the particle-into-liquid sampler (PILS) for ground and airborne measurements of water soluble aerosol composition. Atmospheric Environment 37:1243–1259; doi:10.1016/S1352-2310(02)01015-4.

Peters A, Dockery DW, Muller JE, Mittleman MA. 2001. Increased Particulate Air Pollution and the Triggering of Myocardial Infarction. Circulation 103:2810 –2815; doi:10.1161/01.CIR.103.23.2810.

Pöschl U. 2005. Atmospheric Aerosols: Composition, Transformation, Climate and Health Effects. Angewandte Chemie International Edition 44:7520–7540; doi:10.1002/anie.200501122.

Prousek J. 2007. Fenton chemistry in biology and medicine. Pure and Applied Chemistry 79:2325–2338; doi:10.1351/pac200779122325.

Rattanavaraha W, Rosen E, Zhang H, Li Q, Pantong K, Kamens RM. 2011. The reactive oxidant potential of different types of aged atmospheric particles: An outdoor chamber study. Atmospheric Environment 45:3848–3855; doi:10.1016/j.atmosenv.2011.04.002.

Rhoden CR, Wellenius GA, Ghelfi E, Lawrence J, González-Flecha B. 2005. PM-induced cardiac oxidative stress and dysfunction are mediated by autonomic stimulation. Biochim. Biophys. Acta 1725:305–313; doi:10.1016/j.bbagen.2005.05.025.

Ritz B, Yu F, Fruin S, Chapa G, Shaw GM, Harris JA. 2002. Ambient Air Pollution and Risk of Birth Defects in Southern California. American Journal of Epidemiology 155:17 –25; doi:10.1093/aje/155.1.17.

Sameenoi Y, Mensack MM, Boonsong K, Ewing R, Dungchai W, Chailapakul O, et al. Poly(dimethylsiloxane) cross-linked carbon paste electrodes for microfluidic electrochemical sensing. Analyst 136:3177–3184; doi:10.1039/C1AN15335H.

Schafer FQ, Buettner GR. 2001. Redox environment of the cell as viewed through the redox state of the glutathione disulfide/glutathione couple. Free Radical Biology and Medicine 30:1191–1212; doi:10.1016/S0891-5849(01)00480-4.

Schlesinger RB. 2007. The Health Impact of Common Inorganic Components of Fine Particulate Matter (PM2.5) in Ambient Air: A Critical Review, Inhalation Toxicology, Informa Healthcare. Available: http://informahealthcare.com/doi/abs/10.1080/08958370701402382 [accessed 1 February 2012].

Senn S, Stevens L, Chaturvedi N. 2000. Repeated measures in clinical trials: simple strategies for analysis using summary measures. Statistics in Medicine 19:861–877; doi:10.1002/(SICI)1097-0258(20000330)19:6<861::AID-SIM407>3.0.CO;2-F.

Sioutas C, Delfino RJ, Singh M. 2005. Exposure Assessment for Atmospheric Ultrafine Particles (UFPs) and Implications in Epidemiologic Research. Environ Health Perspect 113:947–955; doi:10.1289/ehp.7939.

Squadrito GL, Cueto R, Dellinger B, Pryor WA. 2001. Quinoid redox cycling as a mechanism for sustained free radical generation by inhaled airborne particulate matter. Free Radical Biology and Medicine 31:1132–1138; doi:10.1016/S0891-5849(01)00703-1.

Stephen A. Wise, Robert L. Watters. 2009. Certificate of Analysis; Standard Reference Material 1649b; Urban Dust.

Stone PH, Godleski JJ. 1999. First steps toward understanding the pathophysiologic link between air pollution and cardiac mortality. American Heart Journal 138:804–807; doi:10.1016/S0002-8703(99)70002-5.

Sullivan AP, Weber RJ, Clements AL, Turner JR, Bae MS, Schauer JJ. 2004. A method for on-line measurement of water-soluble organic carbon in ambient aerosol particles: Results from an urban site. Geophysical Research Letters 31:L13105; doi:10.1029/2004GL019681.

Tamagawa E, Bai N, Morimoto K, Gray C, Mui T, Yatera K, et al. 2008. Particulate matter exposure induces persistent lung inflammation and endothelial dysfunction. Am. J. Physiol. Lung Cell Mol. Physiol. 295:L79–85; doi:10.1152/ajplung.00048.2007.

Timonen KL, Vanninen E, Hartog J de, Ibald-Mulli A, Brunekreef B, Gold DR, et al. 2006. Effects of ultrafine and fine particulate and gaseous air pollution on cardiac autonomic control in subjects with coronary artery disease: The ULTRA study. Journal of Exposure Science and Environmental Epidemiology 16:332–341; doi:10.1038/sj.jea.7500460.

Truong H, Lomnicki S, Dellinger B. 2010. Potential for Misidentification of Environmentally Persistent Free Radicals as Molecular Pollutants in Particulate Matter. Environ. Sci. Technol. 44:1933–1939; doi:10.1021/es902648t.

Venkatachari P, Hopke PK. 2008. Development and Laboratory Testing of an Automated Monitor for the Measurement of Atmospheric Particle-Bound Reactive Oxygen Species (ROS). Aerosol Science and Technology 42:629–635; doi:10.1080/02786820802227345.

Veronesi B, Oortgiesen M, Carter JD, Devlin RB. 1999. Particulate Matter Initiates Inflammatory Cytokine Release by Activation of Capsaicin and Acid Receptors in a Human Bronchial Epithelial Cell Line. Toxicology and Applied Pharmacology 154:106–115; doi:10.1006/taap.1998.8567.

Vidrio E, Phuah C, Dillner AM, Anastasio C. 2009. Generation of Hydroxyl Radicals from Ambient Fine Particles in a Surrogate Lung Fluid Solution. Environ Sci Technol 43: 922–927.

Vizcaya-Ruiz A De, Gutiérrez-Castillo ME, Uribe-Ramirez M, Cebrián ME, Mugica-Alvarez V, Sepúlveda J, et al. 2006. Characterization and in vitro biological effects of concentrated particulate matter from Mexico City. Atmospheric Environment 40, Supplement 2:583–592; doi:10.1016/j.atmosenv.2005.12.073.

Wang Y, Hopke PK, Sun L, Chalupa DC, Utell MJ. 2011. Laboratory and Field Testing of an Automated Atmospheric Particle-Bound Reactive Oxygen Species Sampling-Analysis System. Journal of Toxicology 2011:1–9; doi:10.1155/2011/419476.

Watkinson WP, Campen MJ, Costa DL. 1998. Cardiac Arrhythmia Induction After Exposure to Residual Oil Fly Ash Particles in a Rodent Model of Pulmonary Hypertension. Toxicol. Sci. 41:209–216; doi:10.1093/toxsci/41.2.209.

Wu W, Graves LM, Jaspers I, Devlin RB, Reed W, Samet JM. 1999. Activation of the EGF receptor signaling pathway in human airway epithelial cells exposed to metals. Am J Physiol Lung Cell Mol Physiol 277: L924–L931.

APPENDIX A

Standard Operating Procedures; Chamber Test

1.0 PRE TEST

1.1. Aerosol Chamber

1.1.1. Turn on SMPS; allow the machine to warm up.

1.1.2. NIST – Fill the Collision nebulizer with 60 mL of DI water and ~ 0.6 g urban dust.

1.1.2.1. Sonicate for at least 60 minutes.

1.1.3. Place DustTrak inside aerosol chamber.

1.1.3.1. Turn on DustTrak.

1.1.3.2. Set to data-log at 1 minute intervals. Begin recording.

1.1.4. Turn on desk fan.

1.1.5. Set the nebulizer in the aerosol chamber.

1.1.5.1. Turn on nebulizer to 10 psi (3.5 L/min).

1.1.5.2. Regulate nebulizer with automated on/off switch.

1.1.6. Turn on dilution and exhaust lines to equal flows.

1.1.6.1. Adjust until desired aerosol concentration is reached.

1.1.7. Begin SMPS scans using *standard mode.*

1.2. TRADITIONAL

1.2.1. Pre-weigh 5 filters (3 samples, 2 blanks).

1.2.2. Load sample filters into cassette holders.

1.2.3. Turn on sample manifold.

1.2.3.1. Attach cassettes to sample manifold.

1.2.3.2. Leak test sampling trains.

1.2.3.3. Set sampling flows to 10 L/min or 20 L/min.

1.2.3.4. Pre-measure sampling flows using DryCal.

1.2.3.5. Attach HEPA filters to cassette inlets.

1.3. ON-LINE

1.3.1. Prepare buffers.

1.3.2. 100 mM sodium phosphate buffer, pH 7.0

1.3.2.1. 2.3663 g Na_2HPO_4 (anhydrous) + 1.459 g NaH_2PO_4 + 250 mL DI water.

1.3.2.2. Adjust to pH 7.0 with NaOH solution.

1.3.3. 100 mM sodium phosphate buffer, pH 7.4

1.3.3.1. 3.1743 g Na_2HPO_4 (anhydrous) + 0.7793 g NaH_2PO_4 + 250 mL DI water.

1.3.3.2. Adjust to pH 7.4 with NaOH solution.

1.3.4. Turn on syringe pump.

1.3.4.1. Load 7.0 pH buffer into syringe.

1.3.4.2. Secure syringe onto syringe pump holder.

1.3.4.3. Begin pumping at 60 µL/min.

1.3.5. Turn peristaltic pump on at setting 2 (1.5 mL/min).
1.3.6. Pump DI water into PILS steam injector and onto impaction plate.
1.3.7. Turn on PILS; allow the machine to warm up.
1.3.7.1. Attach HEPA filter to inlet.
1.3.8. Prepare a 40 mL reagent solution containing 50 µM DTT and 100 µM NaF using 7.4 pH buffer.
1.3.9. Prepare 4 mL reagent solutions for calibration curve containing 30, 40, and 60 µM DTT and 100 µM NaF.
1.3.10. Pump 50 µM DTT reagent solution to PILS impaction plate.
1.3.11. Collect 500 second reagent samples into bullet tubes for IC analysis.
1.3.12. Turn on air pump to 13 L/min.
1.3.12.1. Measure flow at PILS inlet using DryCal.
1.3.13. Turn on potentiostat.
1.3.13.1. Run *Cyclic Voltammetry* using the following settings;
1.3.13.1.1. Initial Voltage = -0.1
1.3.13.1.2. High Voltage = 1
1.3.13.1.3. Low Voltage = -0.1
1.3.13.1.4. Sweep Segments = 10
1.3.13.2. Run *Amperometric IT Curve* using the following settings;
1.3.13.2.1. Initial Voltage = 0.2
1.3.13.2.2. Sampling time = 50,000
1.3.13.3. Turn injection valve at ~3 minute intervals until peak heights become consistent.
1.3.13.3.1. Collect at least 3 blank peaks.

2.0 EXPERIMENT
2.1. Remove HEPA filters.
2.2. Attach filter cassettes to chamber.
2.3. Attach PILS to chamber.
2.4. TRADITIONAL
2.4.1. Collect urban dust for 180 minutes.
2.4.2. Post-measure flow using DryCal.
2.4.3. Post-weigh filters.
2.5. ON-LINE
2.5.1. Manual chip injections at ~3 minute intervals.
2.5.2. After urban dust reach chip (~18 minutes) inject at least 10 readings.
2.5.3. Stop program, save file.
2.5.4. Detach PILS from chamber
2.5.5. Clean PILS
2.5.5.1. Re-attach HEPA filter.
2.5.5.2. Send DI water to impaction plate for 15 minutes.

2.5.6. DTT Calibration Curve.

2.5.6.1. Repeat *Cyclic Voltammetry* and *Amperometric IT Curve* programs.

2.5.6.2. Fill syringes with 2 mL of 30, 40, 50, and 60 µM DTT and 100 µM NaF solutions.

2.5.6.3. Reconfigure system for direct flow-injection analysis.

2.5.6.4. Attach syringes (starting with the lowest DTT concentration) and inject onto chip.

2.5.6.5. Obtain 3 consistent peaks for each DTT concentration.

2.5.6.6. Stop program, save file.

2.5.6.7. Clean Chip.

2.5.6.7.1. Replace 7.0 pH syringe buffer with DI water.

2.5.6.7.2. Rinse chip until waste reservoir fills at least 3 times.

3.0 POST-TEST

3.1. Turn off SMPS.

3.2. Turn off DustTrak.

3.3. Turn off nebulizer.

3.4. Clean nebulizer and dry on rack.

3.5. Turn off dilution air.

3.6. Turn off desk fan.

3.7. Turn off exhaust lines.

3.8. Turn of sample manifold.

3.9. Open hood exhaust.

3.10. Turn off air pump.

3.11. Turn off peristaltic pump.

3.12. Turn off PILS.

3.13. Turn off potentiostat.

3.14. Turn off syringe pump.

3.15. Properly dispose of excess reagents/solutions in hazardous waste container.

APPENDIX B

Standard Operating Procedures; Traditional DTT Assay

1.0 PRE-TEST

1.1. Extract Filters.

1.1.1. Arrange and label one 15 mL centrifuge tube for each filter.

1.1.2. Submerge filter and 3 mL methanol in appropriate centrifuge tube.

1.1.3. Place centrifuge tubes in sonicator and cover with tin foil.

1.1.4. Sonicate for 90 minutes.

1.1.5. Cool at room temperature for 60 minutes.

1.1.6. Syringe filter extracts.

1.1.6.1. Perform in fume hood.

1.1.6.2. Attach syringe filter to sterile syringe pump nozzle.

1.1.6.3. Pour extract and filter into syringe pump.

1.1.6.4. Push through syringe filter into clean centrifuge tube.

1.1.7. Concentrate Extracts.

1.1.7.1. Measure and record centrifuge tube + extract pre-mass.

1.1.7.2. In fume hood, prepare 25°C water bath.

1.1.7.3. Stand centrifuge tube in water bath. Open cap.

1.1.7.4. Open N_2 canister to ~10 psi (3.5 L/min).

1.1.7.5. Blow N_2 across extract surface for ~10 minutes.

1.1.7.6. Close centrifuge tube, measure and record post-mass.

1.2. Prepare Stock Solutions

1.2.1. Make in fume hood.

1.2.2. Wear safety glasses, nitrile gloves, and lab coat.

1.2.3. Check pH of all buffers daily.

1.2.4. 10% w/v Trichloroacetic Acid (TCA)

1.2.4.1. 14 g TCA solid + 126 mL Milli-Q water.

1.2.5. 0.1 M Phosphate Buffer, pH 7.4.

1.2.5.1. 11.0478 g Na_2HPO_4 + 3.0205 g KH_2PO_4 + 1 L Milli-Q water.

1.2.5.2. Chelex-treat to remove trace metals. Pour buffer into column with rinsed Chelex beads and drain into glass jar.

1.2.6. 0.4 M Tris Buffer with 20mM EDTA, pH 8.9.

1.2.6.1. 1.041g Tris-HCl + 0.93805 g EDTA + 5.257g Tris Base + 126 mL Milli-Q water.

1.2.7. 10mM Dithiobisnitrobenzoic acid (DTNB).

1.2.7.1. 0.0396 g DTNB + 10 mL Chelex-treated buffer.

1.2.7.2. Immediately cover with aluminum foil.

1.2.8. 4 mM Dithiothreitol (DTT).

1.2.8.1. 0.0154 g DTT + 25 mL Chelex-treated buffer.

1.2.9. 100 µM DTT Dilution (reactant).

1.2.9.1. 1.8702 mL of 4 mM DTT stock + 75 mL Chelex-treated buffer.
1.2.9.2. Immediately cover with aluminum foil.
1.2.10. Make 1 mL serial dilutions from 100 µM DTT solution for calibration curve.
1.2.10.1. 90, 80, 70, 60, and 50 µM DTT.
1.2.10.2. Dilute with Chelex-treated buffer.
1.2.10.3. Add 200 µL methanol, mix well.
1.2.11. 2.5 µg/100µL 1,4 Naphthaquinone (1,4 NQ) dilution (quality control).

2.0 EXPERIMENT

2.1. Place 37°C water bath on hot plate.
2.2. Prepare quenching vials.
2.2.1. Add 250 µL of 10% TCA to quenching vials.
2.2.2. Group vials by time point.
2.2.3. Cover with aluminum foil.
2.2.4. Quench the zero time point.
2.2.4.1. Add 41.7 µL methanol and 208.3 µL of 100 µM DTT stock to quenching vials.
2.2.5. Quench DTT dilutions for calibration curve.
2.2.5.1. Same procedure as zero time point.
2.3. Start reaction.
2.3.1. Add 100 µL urban dust or blank extract to 500 µL DTT in a test tube.
2.3.2. Place test tubes in water bath, cover with aluminum foil.
2.3.3. Begin stopwatch.
2.3.4. At 5 and 10 minutes, remove and quench 250 µL of the reaction volume.
2.3.4.1. Use new pipette tip for each sample.
2.3.4.2. Immediately cover with aluminum foil.
2.3.4.3. Solutions stable for ~2 hrs. in the dark.
2.3.5. Add 25 µL DTNB to quenched solutions.
2.3.5.1. Mix well.
2.3.5.2. Allow to react for 1 minute.
2.3.6. Add 1 mL of 0.4M Tris buffer to quenched solutions.
2.4. Absorbance analysis.
2.4.1. Turn on spectrophotometer.
2.4.2. Set to *Absorbance Scan*.
2.4.3. Read at 412 nm.
2.4.4. Move quenched solutions to cuvette.
2.4.5. Measure and record absorbance, three readings .
2.5. Quality control.
2.5.1. Repeat experiment with 100 µL 2.5 µg/100µL 1,4 NQ instead of urban dust.
2.5.2. Results valid if 1,4 Naphthaquinone consumes DTT between 11-15 nmol DTT/min/µg 1,4 Naphthaquinone.

3.0 POST-TEST

3.1. Turn off spectrophotometer.
3.2. Properly dispose of hazardous waste.
3.3. Clean glassware and dry on rack.
    3.3.1. Dispose of glassware in designated broken glass container.

APPENDIX C

SAS Code

```
data react;

input assay $ rep $ chip $ conc $ meas_conc assay_meas_conc sample $
reactivity reactivity_adj;
      *Input data, '$' signifies categorical variable

datalines;
Traditional N90R1 T High 69.352 9.610 1N90 328.516 34.183
Traditional N90R1 T High 69.352 7.426 2N90 549.042 73.936
Traditional N90R1 T High 69.352 6.433 3N90 339.883 52.837
Online N90R1      A High 69.352 0.068 A 7.879 115.626
Online N90R1      A High 69.352 0.068 B 7.213 105.848
Online N90R1      A High 69.352 0.068 C 8.352 122.566
Online N90R1      A High 69.352 0.068 D 7.435 109.106
Traditional N90R2 T High 65.000 9.336 6N90 247.458 26.506
Traditional N90R2 T High 65.000 6.131 7N90 351.141 57.270
Traditional N90R2 T High 65.000 7.684 8N90 378.790 49.298
Online N90R2      A High 65.000 0.066 A 6.398 98.908
Online N90R2      A High 65.000 0.066 B 6.264 96.838
Online N90R2      A High 65.000 0.066 C 6.247 96.579
Online N90R2      A High 65.000 0.066 D 5.812 89.852
Online N90R2      A High 65.000 0.066 E 6.047 93.474
Online N90R2      A High 65.000 0.066 F 7.319 113.139
Online N90R2      A High 65.000 0.066 G 7.402 114.433
Online N90R2      A High 65.000 0.066 H 6.499 100.461
Traditional N90R5 T High 73.519 6.218 1N90R5 415.509 66.820
Traditional N90R5 T High 73.519 4.564 2N90R5 554.011 121.397
Traditional N90R5 T High 73.519 5.067 4N90R5 475.080 93.766
Online N90R5      B High 73.519 0.060 A 6.016 100.847
Online N90R5      B High 73.519 0.060 B 5.686 95.314
Online N90R5      B High 73.519 0.060 C 6.010 100.753
Online N90R5      B High 73.519 0.060 D 5.180 86.844
Online N90R5      B High 73.519 0.060 E 4.396 73.695
Traditional N30R2 T Mid 29.167 3.029 21N30 237.783 78.505
Traditional N30R2 T Mid 29.167 3.307 22N30 243.313 73.573
Traditional N30R2 T Mid 29.167 3.284 23N30 196.309 59.774
Online N30R2      A Mid 29.167 0.028 A 2.300 115.626
Online N30R2      A Mid 29.167 0.028 B 3.130 105.848
Online N30R2      A Mid 29.167 0.028 C 2.004 122.566
Online N30R2      A Mid 29.167 0.028 D 2.706 109.106
Online N30R2      A Mid 29.167 0.028 E 2.824 112.507
Traditional N30R3 T Mid 22.731 2.103 26N30 346.997 165.039
Traditional N30R3 T Mid 22.731 2.261 27N30 289.625 128.122
Traditional N30R3 T Mid 22.731 2.460 28N30 358.057 145.571
Online N30R3      A Mid 22.731 0.024 A 2.612 109.141
Online N30R3      A Mid 22.731 0.024 B 2.956 123.503
Online N30R3      A Mid 22.731 0.024 C 2.149 89.775
Online N30R3      A Mid 22.731 0.024 D 2.638 110.189
Traditional N30R4 T Mid 27.062 2.456 1N30R4 331.091 134.798
Traditional N30R4 T Mid 27.062 2.173 2N30R4 437.734 201.461
Traditional N30R4 T Mid 27.062 4.010 3N30R4 138.885 34.634
Online N30R4      B Mid 27.062 0.020 A 2.907 140.882
```

```
Online N30R4       B Mid 27.062 0.020 B 2.442 118.351
Online N30R4       B Mid 27.062 0.020 C 3.069 148.736
Online N30R4       B Mid 27.062 0.020 D 2.831 137.233
Online N30R4       B Mid 27.062 0.020 E 3.349 162.342
Online N30R4       B Mid 27.062 0.020 F 2.720 131.852
Online N30R4       B Mid 27.062 0.020 G 2.813 136.336
Online N30R4       B Mid 27.062 0.020 H 2.961 143.510
Traditional N10R5 T Low 17.953 3.928 1N10R5 225.680 57.456
Traditional N10R5 T Low 17.953 4.848 3N10R5 156.240 32.227
Traditional N10R5 T Low 17.953 2.412 4N10R5 298.840 123.907
Online N10R5       B Low 17.953 0.014 A 1.028 75.085
Online N10R5       B Low 17.953 0.014 B 1.684 123.057
Online N10R5       B Low 17.953 0.014 C 1.268 92.623
Online N10R5       B Low 17.953 0.014 D 1.488 108.729
Online N10R5       B Low 17.953 0.014 E 2.118 154.737
Online N10R5       B Low 17.953 0.014 F 1.834 134.008
Online N10R5       B Low 17.953 0.014 G 2.208 161.309
Online N10R5       B Low 17.953 0.014 H 0.904 66.049
Online N10R5       B Low 17.953 0.014 I 2.654 193.911
Traditional N10R8 T Low 21.961 3.932 1N10R8 182.551 46.425
Traditional N10R8 T Low 21.961 3.937 2N10R8 152.948 38.845
Traditional N10R8 T Low 21.961 1.916 3N10R8 133.213 69.538
Online N10R8       B Low 21.961 0.016 A 3.615 219.410
Online N10R8       B Low 21.961 0.016 B 3.254 197.543
Online N10R8       B Low 21.961 0.016 C 3.080 186.962
Online N10R8       B Low 21.961 0.016 D 2.253 136.746
Online N10R8       B Low 21.961 0.016 E 1.349 81.867
Online N10R8       B Low 21.961 0.016 F 0.321 19.490
Online N10R8       B Low 21.961 0.016 G 0.132 8.028
Online N10R8       B Low 21.961 0.016 H 1.291 78.381
Traditional N10R7 T Low 14.996 2.830 1N10R7 272.189 96.183
Traditional N10R7 T Low 14.996 2.537 2N10R7 200.887 79.194
Traditional N10R7 T Low 14.996 4.187 3N10R7 160.585 38.353
Online N10R7       B Low 14.996 0.011 A 0.638 52.081
Online N10R7       B Low 14.996 0.011 B 1.301 106.091
Online N10R7       B Low 14.996 0.011 C 0.579 47.266
Online N10R7       B Low 14.996 0.011 D 3.594 293.143
Online N10R7       B Low 14.996 0.011 E 2.403 196.062
run;

proc print data=react;run;
      *Ensure data input correctly

proc reg data=react;
 model reactivity=meas_conc / clb;
      *Regress raw DTT consumption rate against chamber PM mass, 'clb' shows
      intercept significance
 model reactivity=assay_conc / clb;
      *Regress raw DTT consumption rate against assayed PM mass for each
      method
 by assay;
      *Separate regression by method type for qualitative comparison
run;
```

```
proc corr data=react;
 var meas_conc assay_meas_conc reactivity;
      *Pearson correlation between PM mass and raw DTT consumption rate
 by assay;
      *Separate correlation by method type for qualitative comparison
run;


proc mixed data=react2; class assay rep chip conc;
      *Class variables specify categorical analysis
 model reactivity_adj = assay|conc chip(assay)/outp=residuals;
      *Interaction term between assay and concentration permits pairwise
      comparisons later
      *'chip(assay)' tests for differences between the two on-line systems

 random rep(conc) assay*rep*conc;
      *Account for repeated measures and unbalanced nature of on-line data
      compared to corresponding traditional data
 lsmeans assay|conc chip(assay)/pdiff;
      *Pairwise comparisons between groups
run;

proc plot data=residuals;
 plot resid*pred;
      *Residual analysis for mixed model
run;
```